CROSS-STRUCTURAL DEVELOPMENT AT THE SOUTHWESTERN TERMINATION OF WALKER MOUNTAIN, VIRGINIA

by

David J. Monz

Thesis submitted to the Faculty of the

Virginia Polytechnic Institute and State University

in partial fulfillment of the requirements for the degree of

Master of Science

in

Geological Sciences

APPROVED:

Lynn Glover, III, Chairman

Wallace D. Lowry

J. Fred Read

August, 1985

Blacksburg, Virginia

CROSS-STRUCTURAL DEVELOPMENT AT THE SOUTHWESTERN TERMINATION OF WALKER MOUNTAIN, VIRGINIA

by

David J. Monz

Lynn Glover, III, Chairman

Geological Sciences

(ABSTRACT)

The Saltville thrust sheet in the southwest Virginia portion of the Appalachian foreland fold and thrust belt generally has very little penetrative deformation. At the southern termination of Walker Mountain however, a continuous 10-15 km zone along strike is highly strained and polydeformed. In this area a NW-trending mesoscopic solution cleavage and associated buckle folds are obliquely superimposed on the regional northeast structural trend. Values of penetrative strain, determined from syntectonic fibrous mineral growths in pressure fringes, vary along strike and vertically within the thrust sheet and indicate up to 50% shortening approximately orthogonal to cleavage. Fibers are virtually straight and undeformed reflecting a nearly coaxial strain history associated with cross-structural evolution.

The cross-structures deform the Saltville sheet as well as the leading edge of the Pulaski sheet and were not rotated into their present orientation, but were initiated and evolved oblique to the northwest direction of tectonic

transport. Cross-structural development is best explained by the oblique propagation of a portion of the frontal-tip of the evolving Saltivlle thrust in response to varying degrees of detachment. The variable ease with which the decollement was able to migrate through the rocks created zones of differential movement in the overlying sheet and the generation of locally high strains in the tip region. Spatial variation in strain and in the orientation of structural elements may be used to delineate zones of differential thrust movement.

ACKNOWLEDGEMENTS

The author gratefully acknowledges Dr. Lynn Glover, III, not only for his help and encouragement throughout the study, but also for providing the opportunity to explore various aspects of geology that would otherwise have been impossible. Dr. Wallace D. Lowry introduced the author to the Valley and Ridge Province of Virginia and provided unparalled inspiration through his dedication to the science of geology and education of students.

Appreciation is extended to Drs. Stewart S. Farrar and J. Fred Read for their critical reading of and constructive comments on the preliminary draft, Dr. Arthur P. Schultz and Charles Stanley for numerous discussions on the local structural geology and to Kathy Hawkins for drafting the figures and the final map. Dr. Lucian W. Zelazny and Willie Harris gave generously of their time and expertise during the clay mineralology analysis. A personal thanks is extended to Marge Dellers for her helpful advice, friendship and the maintainance of order during the study.

Financial support was provided through a graduate teaching assistantship from Virginia Polytechnic Institute and State University and through a contract with Sohio Petroleum entitled "Reflection Seismic Studies in Virginia" which was awarded to Drs. John K. Costain, Lynn Glover, III and Cahit Coruh.

A very special thanks is expressed to the author's parents, Joseph and Dorothy Monz, for continuous moral and financial support when times were tough, and to Elizabeth Trayner for her endless patience and support throughout the study.

TABLE OF CONTENTS

LIST OF ILLUSTRATIONS

INTRODUCTION

Thin-skinned tectonic models describing the structural development of foreland fold and thrust belts frequently regard thrust sheets as rigid rock masses. However, thrust sheets are not completely rigid plates and may show complex internal deformation and complex strain histories due to differential movements within the sheet.

The ease with which decollement propagates may vary for a particular thrust surface, resulting in the development of locally high strains in the tip region. The orientation and type of strain will vary depending on the relative contributions of frontal- and lateral-tip components (Coward and Potts, 1983, Kligfield, 1983). Strain may vary along strike (Coward, 1982, Fischer and Coward, 1982, Rattey and Sanderson, 1982, Sanderson, 1982, Coward and Potts, 1983) and vertically within the sheet (Elliot, 1976, Sanderson, 1982, Wojtal, 1982, Ramsay et al., 1983) in response to differential internal movements during thrust sheet emplacement. Differential transport may lead to the development of structures oriented obliquely to the regional structural trend. Such structures have recently been studied by Coward and Kim (1981), Fisher and Coward (1982) and Coward and Potts (1983) in parts of Scotland. These workers have commonly attributed the oblique structural attitude to the rotation of earlier formed structures in response to layer normal shear due to differential thrust movement. Beach (1982) considers similar cross-structures to have evolved by the synchronous addition of layer parallel shortening and layer normal shear.

This paper discusses the development of NW-trending cross-structures which are obliquely superimposed on the regional southern Appalachian structural trend in a portion of the Saltville thrust sheet of southwestern Virginia. Variations in the geometric relations of structural elements, in strain patterns and in the relative deformation chronology are used to interpret the progressive evolution of the cross-structures during thrust sheet emplacement.

GEOLOGIC SETTING

The southern portion of the Appalachian foreland fold and thrust belt is characterized by linear to arcuate belts of deformed Paleozoic strata which have been transported northwestward on NE-SW trending thrust faults (Figure 1). Major thrusts have strike lengths of up to 700 km with horizontal displacements ranging from 10 to 50 km (Gwinn, 1970, Harris, 1970, Rodgers, 1970, Lowry, 1971, Bartholomew, 1979) and generally climb section in the direction of tectonic transport (Rich, 1934). Thrusts typically display listric to step-like geometry and merge with a master decollement in the Cambrian Rome Formation at depth (Harris and Milici, 1977, Harris and Bayer, 1979, Boyer and Elliot, 1982). Displacement is commonly transferred to terminal anticlinoria and/or imbricate thrust slices at lateral tips (House and Gray, 1982). Relative initiation of folds versus thrusts may vary, but the close association of thrust faults and regional folds implies a genetic relationship. Regional footwall synclines (cf. Roeder et al., 1978b, Stanley, 1983) appear to be active folds (cf. Harris and Milici, 1977) which necessitates that the initiation of folding be prior to, or synchronous with, thrust propagation (Lowry, 1979, Fischer and Coward, 1982). Structural relations between thrust sheets suggest a general age progression of structural de-

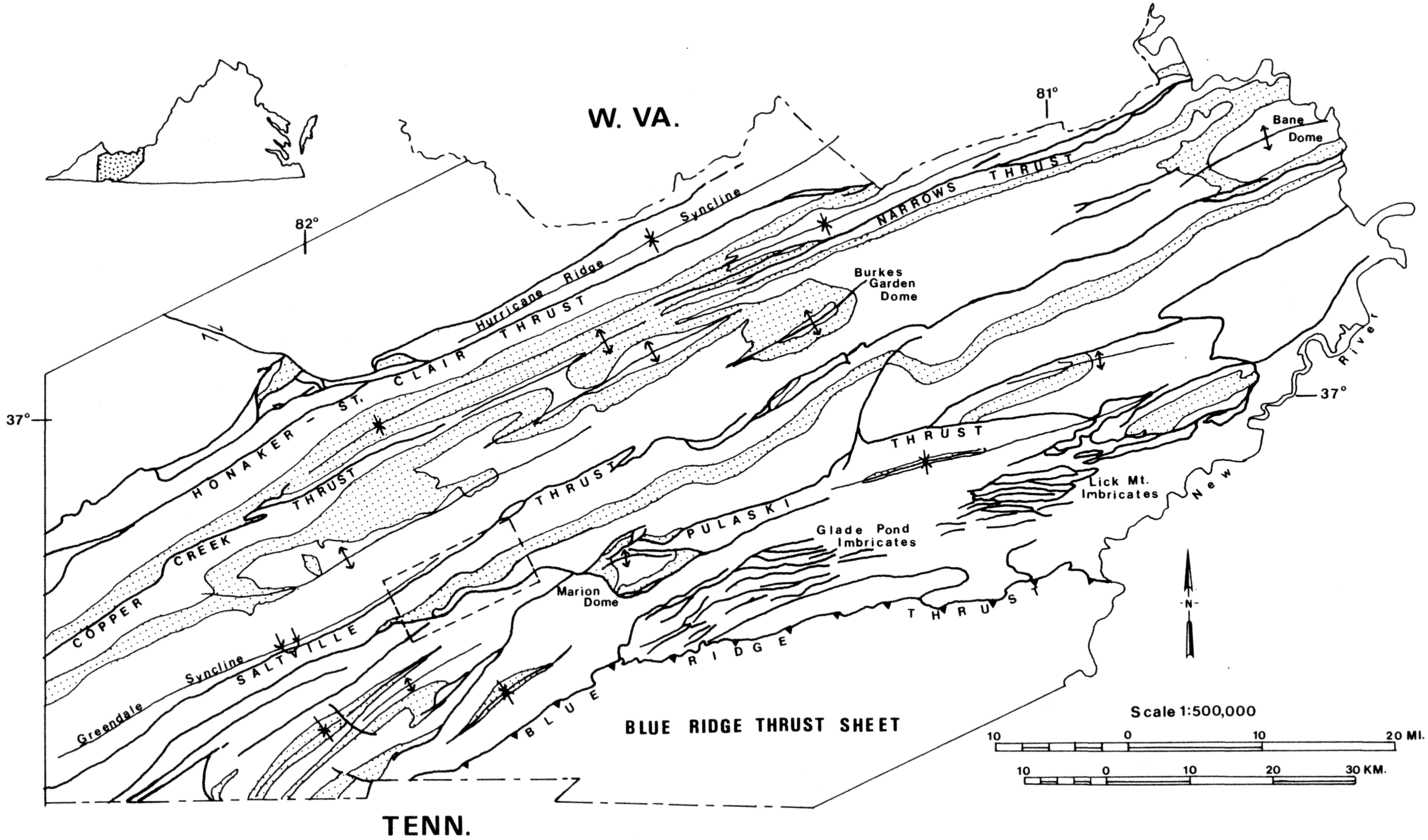

Figure 1. Regional tectonic index map, southwestern Virginia (modified from Calver, 1963).: Middle Ordovician carbonate units are stippled. Dashed rectangle shows area of Figure 3.

velopment becoming younger toward the NW (cratonward) in the direction of tectonic transport (Perry, 1978, Burchfiel, 1980).

The area studied contains portions of two regional thrust sheets: the Saltville on the northwest and the Pulaski-Walker Mountain on the southeast (Figure 2). Both faults thrust dominantly Cambro-Ordovician carbonates over deformed footwall strata ranging in age from Ordovician to Mississippian (cf. Schultz, 1979, 1983). The Saltville sheet and the leading edge of the Pulaski-Walker Mountain sheet are polydeformed in this area. The regional NE-trending Walker Mountain Syncline occupies the footwall of the Pulaski thrust and is structurally overprinted by oblique, cross-cutting, NW-trending folds and a strong spaced solution cleavage.

Internal deformation of the Saltville sheet is variable along strike, ranging from tight, first-order folds and imbricate thrust slices in parts of Tennessee (cf. Roeder et al., 1978a) to a monoclinally dipping succession overlying the decollement in Virginia. Conodont alteration indices (Harris et al., 1978) indicate maximum paleotemperatures of 200-300°C during deformation.

The preserved thickness of the Saltville sheet ranges from approximately 3000 m in the study area to 4500 m along strike (cf. Cooper, 1961, Lowry, 1979). Stratigraphy and regional structure have been previously discussed by Stevenson (1885), Butts (1933, 1940), Butts and Edmundson

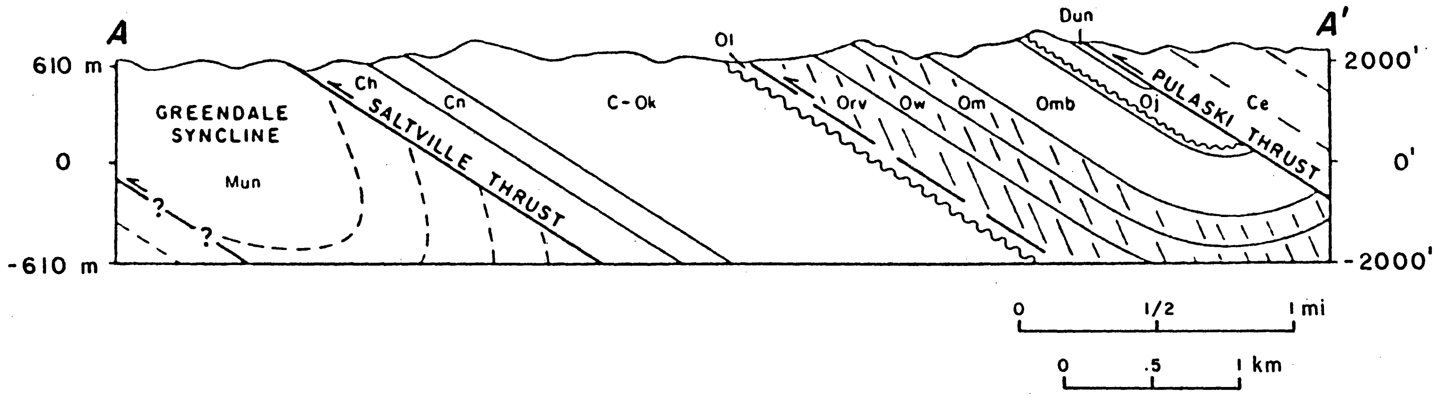

Figure 2b. Geologic map and cross section of the southwestern ternination of Walker Mountain, Smyth and Washington Counties, Virginia.: Location of cross-section A-A' is shown. Abbreviations: Ch Honaker Fm.; Ce=Elbrook Fm.; Cn=Nolichucky Fm.; C-Ok=Knox Gp.; Ot=Tumbez Fm.; Ol=Lenoir Fm.; Oe=Effna Fm.; Orv=Rich Valley Fm.; Ow=Wassum Fm.; Om=Moccasin Fm.; Omb=Martinsburg Fm.; Oj=Juniata Fm.; O-S_s=Ordovician-Silurian sandstones (Juniata and Tuscarora Fms.); Dh=Huntersville Chert; Dun=Devonian undifferentiated (Millboro, Brallier and Chemung Fms.); Mun=Mississippian undifferentiated (Narrows thrust sheet). 31 = strike & dip of bedding; 69 = strike & dip of s_1; 70 = strike and dip of s_2.
Geologic mapping by D. Monz, Lynn Glover, lll and Fred Webb, 1974-1984.

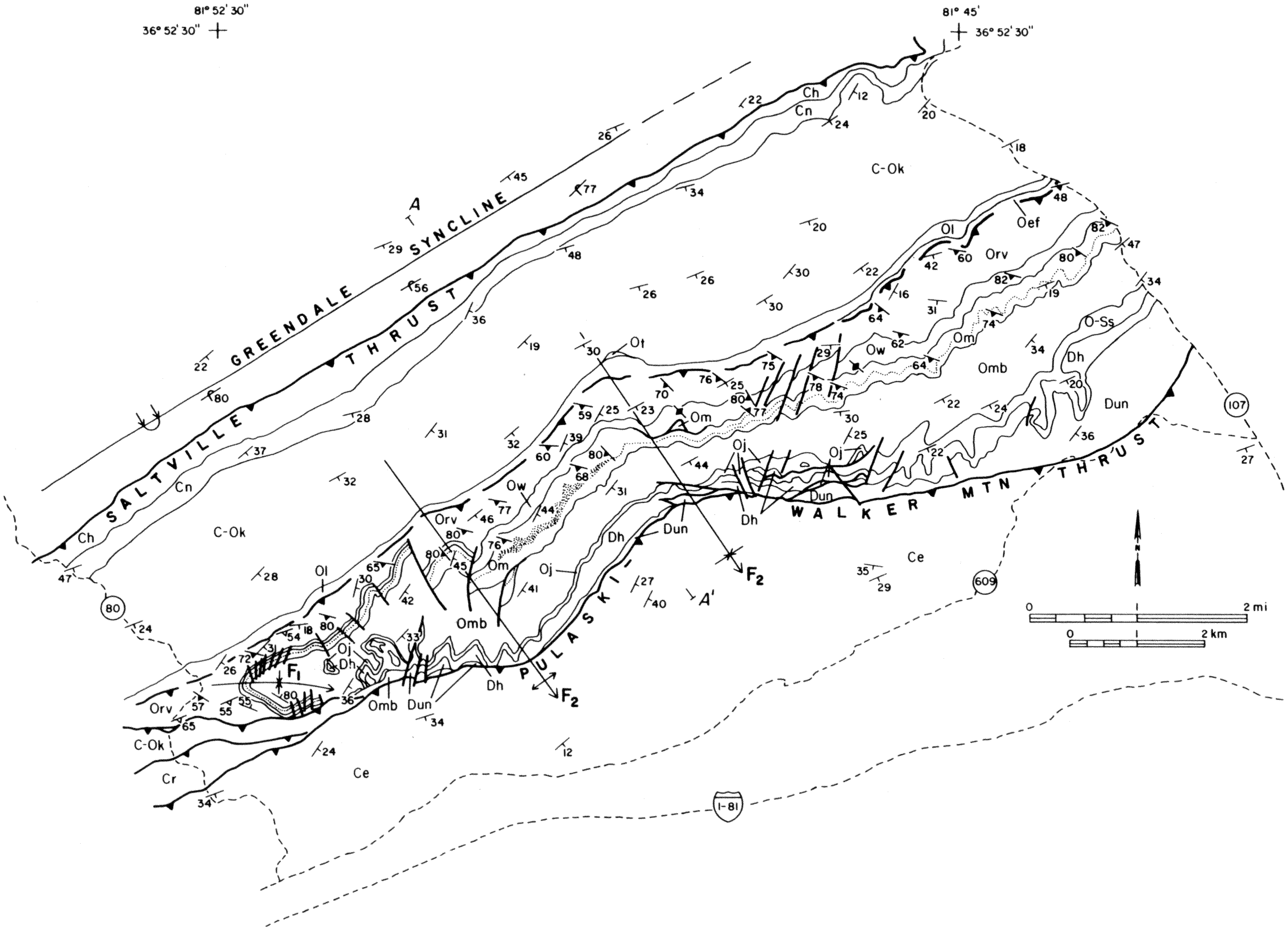
81° 52' 30"
36° 52' 30"
81° 45'
36° 52' 30"
GREENDALE SYNCLINE
SALTVILLE THRUST
WALKER MTN THRUST
PULASKI
A
A'
F1
F2
F2
Ch
Cn
C-Ok
Ol
Oef
Orv
Ow
Om
Omb
O-Ss
Dh
Dun
Oj
Ot
Ce
Cr
107
609
80
I-81
0
2 mi
0
2 km

(1943) and Webb (1959, 1965). The Cambrian through Early Ordovician sequence and the Middle Ordovician sequence of carbonate and clastic rocks (Figure 3) represent respectively the evolution of a passive margin and foreland basin (Read, 1980). Deposition terminated with thrust sheet emplacement during the Alleghanian orogenic episode.

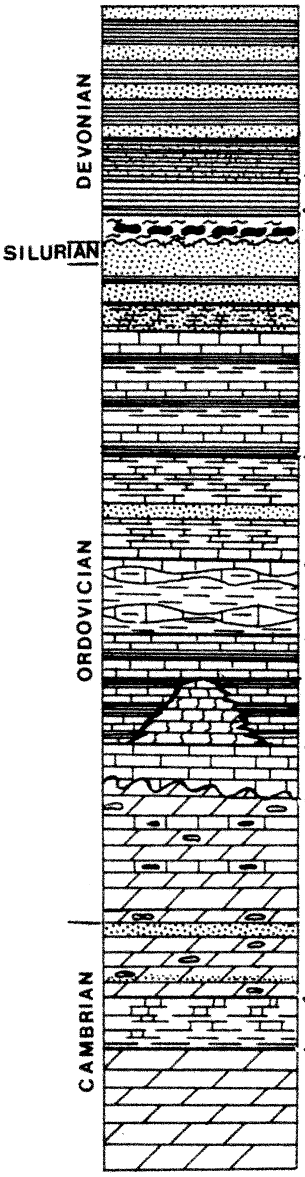

Devonian Undifferentiated (Dun): Brallier Fm.- thin-bedded sandstone and siliceous gray shale (~150 m); Chemung Fm.- medium-bedded sandstone and yellow-brown shale (~305 m).

Millboro Fm. (Dm): black fissile shale (<95 m).

Huntersville Chert (Dh): irregularly bedded, gnarled black chert with sparse sandstone and shale interbeds (~10 m).

UNCONFORMITY- increasing in magnitude from NE to SW

Tuscarora Fm. (St): white to light gray, medium-grained, cross-bedded quartzite (<5 m).

Juniata Fm. (Oj): dark red, medium-bedded sandstone with minor red and green shale and siltstone interbeds (<95 m).

Martinsburg Fm. (Omb): interbedded dark gray, thin-bedded, coarse-grained skeletal limestone, brown sandstone, and yellow-brown shale and siltstone (~485 m).

Moccasin Fm. (Om): red calcareous mudrock, argillaceous limestone and pelletal limestone; locally well developed penetrative to spaced cleavage. Walker Mtn. sandstone member (Omw): white to gray, medium-grained, conglomeratic quartzite (~92 m).

Wassum Fm. (Ow): light gray skeletal grainstone and shaly pelletal to nodular limestone; locally cleaved (~92 m).

Rich Valley Fm. (Orv): black calcareous shale and limestone; locally well developed penetrative to spaced cleavage (~215 m).

Effna Fm. (Oe): light gray skeletal grainstone and wackestone (<30 m)

Lenoir Fm. (Ol): gray, medium- to thick-bedded skeletal grainstone and packstone with silty dolomite stringers (~45 m). Localized gray skeletal grainstone and fine-grained sandstone at base (Ot-Tumbez).

KNOX UNCONFORMITY

Knox Gp. (C-Ok): Lower Knox- gray, thin- to thick-bedded stromatolitic dolomite with minor interbedded sandstones; Upper Knox- gray, medium- to thick-bedded cherty dolomite with limestone interbeds (<900 m).

Nolichucky Fm. (Cn): limestone-dolomite ribbon rock, calcareous shale and siltstone (125 m).

Honaker Fm. (Ch): gray, thick- to massively bedded, fine- to medium-grained dolomite (<450 m exposed in the Saltville sheet).

Figure 3. Generalized stratigraphic column for the Saltville thrust sheet in Smyth and Washington Counties, Virginia.

STRUCTURAL ELEMENTS

Mesoscopic and microscopic deformational features record strain in this portion of the Saltville sheet. Relations between structural elements provide an opportunity to examine the spatial and temporal kinematics of regional structural evolution. Folds, faults, cleavage, veins and kink bands (Figure 4) are discussed individually.

FOLDS

Two distinct fold generations are recognized with the NE-trending regional F_1 Walker Mountain Syncline obliquely overprinted by gentle NW-trending F_2 cross-folds (Figure 5). The broad, gently SE-plunging sub-regional cross-folds affect the structural orientation of units within the Saltville thrust sheet and the leading edge of the Pulaski sheet.

In profile section the F_1 Walker Mountain Syncline is a close, asymmetric, regional fold plunging gently to the northeast. The upright, northwest limb dips 30-40° SE and the steeply dipping to overturned southeast limb is truncated by the Walker Mountain-Pulaski Thrust. A well developed NE-trending slaty cleavage (S_1) sporadically occurs near the base of the Rich Valley Formation in the axial region of the fold. NE-trending F_1 mesoscopic folds, though not common,

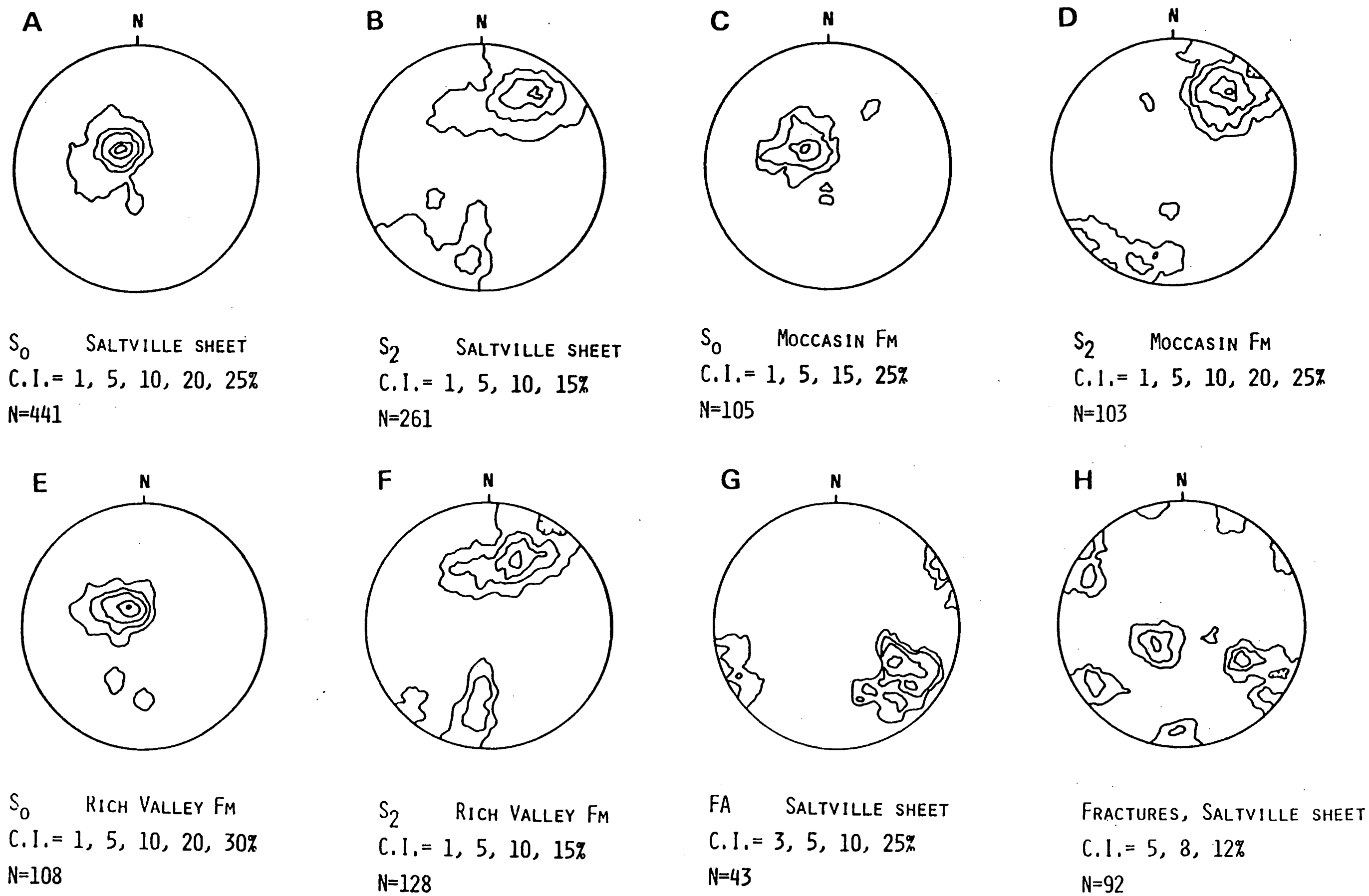

Figure 4. Equal area projections (Wulff stereonets) of structural orientation data- C.I.= contour interval.: a) poles to bedding, Saltville thrust sheet. b) poles to S_2 cleavage. c) poles to bedding, Moccasin Fm. d) poles to S_2 cleavage, Moccasin Fm. e) poles to bedding, Rich Valley Fm. f) poles to S_2 cleavage, Rich Valley Fm. g) mesoscopic fold axes. h) poles to fractures.

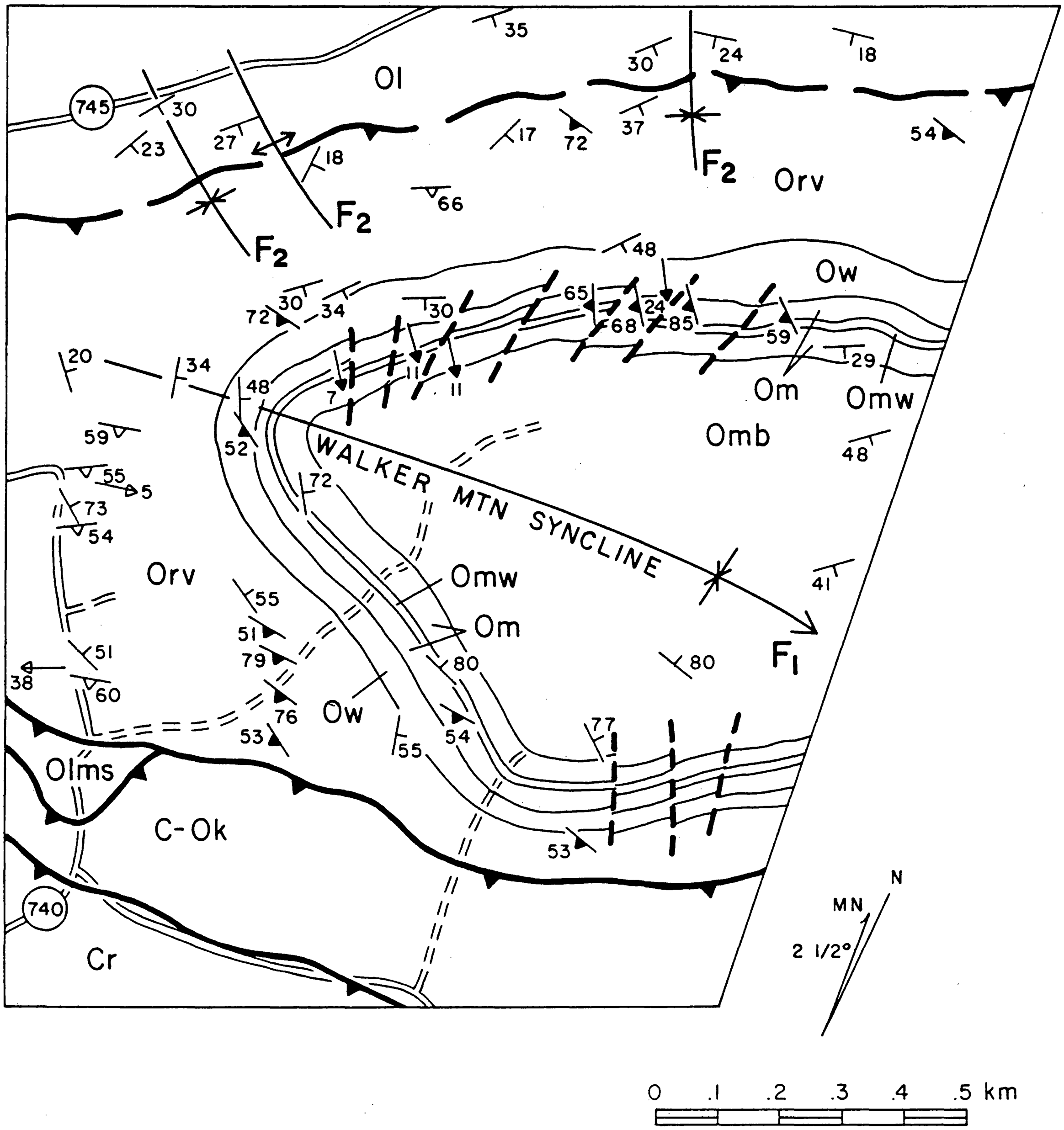

Figure 5. Structural relations at the closure of the Walker Mountain Syncline.

are developed in the axial portion of the fold and on its northwest limb. Fold style varies with lithology and appears to be dependent on layer thickness and on competency contrasts between layers. Folds in competent, medium- to thick-bedded dolomite and limestone are sub-horizontal, gentle to open folds, with wavelengths of 5-40 m and amplitudes of 2-10 m. Fold profiles are symmetric to slightly asymmetric (interlimb angles>120°) with upright to steeply inclined axial surfaces characteristic of class 1B geometry (Ramsay, 1967). F_1 folds in less competent units have similar attitudes but varying styles. Wavelengths range from 1-10 m with amplitudes from 0.3-5 m. Fold geometry is dominantly class 1B/1C with rounded to angular hinges. Near chevron forms occur in thin-bedded, multilayer packages.

Oblique, NW-trending F_2 cross-folds are superimposed on the regional northeast structural trend and deform units of both the Saltville and Pulaski thrust sheets (Figure 2). Folds range in magnitude from mesoscopic to sub-regional. Broad, gentle, low-amplitude, sub-regional folds (wavelengths < 7 km) are evident from lithologic map patterns and the smooth arcs of structural orientation data. Mesoscopic F_2 folds are commonly developed on the northwest limb of the Walker Mountain Syncline in the Rich Valley, Wassum, Moccasin and Martinsburg Formations. These mesoscopic folds are gentle to open, sinusoidal forms with wavelengths of 0.5-20 m and amplitudes of 0.3-5 m. Fold axes plunge gently southeast and axial surfaces are upright to steeply inclined to the southwest and northeast. Fold profiles are symmetric to slightly asymmetric and display class 1B/1C geometry (Ramsay, 1967).

A well developed compound cleavage (cf. Gray, 1981) is associated with the NW-trending F_2 folds in the Rich Valley and Moccasin Formations. The cleavage commonly forms convergent fans about the axial planes of folds, is refracted across lithologic contacts and appears to slightly transect sub-regional F_2 folds.

FAULTS

The study area is characterized by several orders of NE-trending contraction faults (cf. Price, 1967, Simon and Gray, 1982) and by NE- and NW-trending cross-faults.

CONTRACTION FAULTS

Regional (first-order) thrusts are the dominant structural features, with portions of two, the Walker Mountain-Pulaski and the Saltville, exposed in the study area. The base of each thrust sheet is characterized by highly contorted bedding exhibiting disharmonic and polyclinal fold styles in relatively thin-bedded, incompetent units (Cambrian Rome, Mississippian Maccrady Formations). A well developed tectonic breccia occurs sporadically along the trace of the Walker Mountain-Pulaski thrust (cf. Schultz, 1983). Seismic reflection profiling has shown that these faults have listric to step-like geometry and merge with the basal decollement in the Cambrian Rome Formation at depth (Harris and Bayer, 1979, Milici et al., 1979).

Detachment occurs between the competent Mid-Ordovician limestones and incompetent strata of the Ordovician Rich Valley Formation (Figure 2). Although poorly exposed, the contact is strongly deformed by NW-directed thrusting in places and is referred to as a sub-regional (second-order) contraction fault. Strong mesoscopic deformation and a locally developed NE-trending slaty cleavage occur adjacent to zones of detachment.

Mesoscopic (third order) thrusts are evident at outcrop scale in the Ordovician Rich Valley through Martinsburg succession. These are typically bedding-parallel detachments which may ramp-up section and produce broad anticlinal folds in the hanging wall (cf. Morse, 1977, Serra, 1977). Some of these faults are gently folded and/or cut by steeply dipping, third order extension faults.

CROSS-FAULTS

Numerous NE- to NW-trending, nearly vertical, transcurrent faults offset the Ordovician succession of the Rich

Valley to Martinsburg Formations within the Saltville thrust sheet (Figure 2, Figure 5). These cross-faults have a consistent right-lateral sense of offset, with displacements ranging from 1 to 700 m (cf. Butts and Edmundson, 1943). Displacement on the cross-faults cannot be traced into Ordovician formations older than the Rich Valley, therefore detachment near the base of the Rich Valley formation may be inferred. Similar cross-faults identified by Butts and Edmundson (1943) southwest of the study area appear to locally offset the trace of the Walker Mountain-Pulaski thrust.

Structural relationships indicate a close temporal association between the contraction faults and the cross-faults. Second- and third-order contraction faults and cross-faults appear to have evolved during Walker Mountain (F_1) folding. The NW-trending F_2 cross-folds and S_2 cleavage are not affected by the faulting and appear to be related to a separate deformational episode.

CLEAVAGE

Two distinct generations of cleavage are developed in the Saltville sheet at the southwestern end of Walker Mountain in Virginia.

1. A sporadic, but penetrative NE-trending fabric associated with regional F_1 fold development, and

2. a well developed, penetrative to spaced NW-trending compound tectonic fabric related to the F_2 folding event.

Cleavage is best developed in carbonate mudrock and argillaceous limestone of the Mid-Ordovician Rich Valley and Moccasin Formations.

The NE-trending cleavage is preferentially developed near the base of the Rich Valley Formation in the axial zone of the Walker Mountain Syncline and adjacent to NE-trending mesoscopic contraction faults. It is a penetrative fabric and is deformed by subsequent folding and faulting (Figure 6). The NW-trending fabric (S_2) is the dominant cleavage in the area (Figure 7). Cleavage morphology is dependent on lithology and strain state and ranges from a near slaty type in calcareous mudrock to a compound tectonic fabric (Gray, 1981) in argillaceous limestone. The compound fabric is characterized by the existence of two approximately coplanar tectonic anisotropies, with a penetrative domainal microfabric preserved in the lithons of a more widely spaced, smooth stylolitic form (see 'Microstructure').

Figure 6. NE-trending S_1 cleavage in the Rich Valley Formation.: a) S_1 slaty cleavage near the base of the Rich Valley Formation. b) Kinking and fracturing of the S_1 slaty cleavage. c) Micro-folding of the S_1 cleavage in the axial zone of Walker Mountain Syncline. Lens cap is 5 cm in diameter. d) Photomicrograph of stylolitic axial planar crenulation cleavage associated with the micro-folds shown in (a). NE-trending S_1 domainal micro-fabric is sub-horizontal, NE-trending crenulations dip steeply from upper left to lower right. Bar scale=100μ.

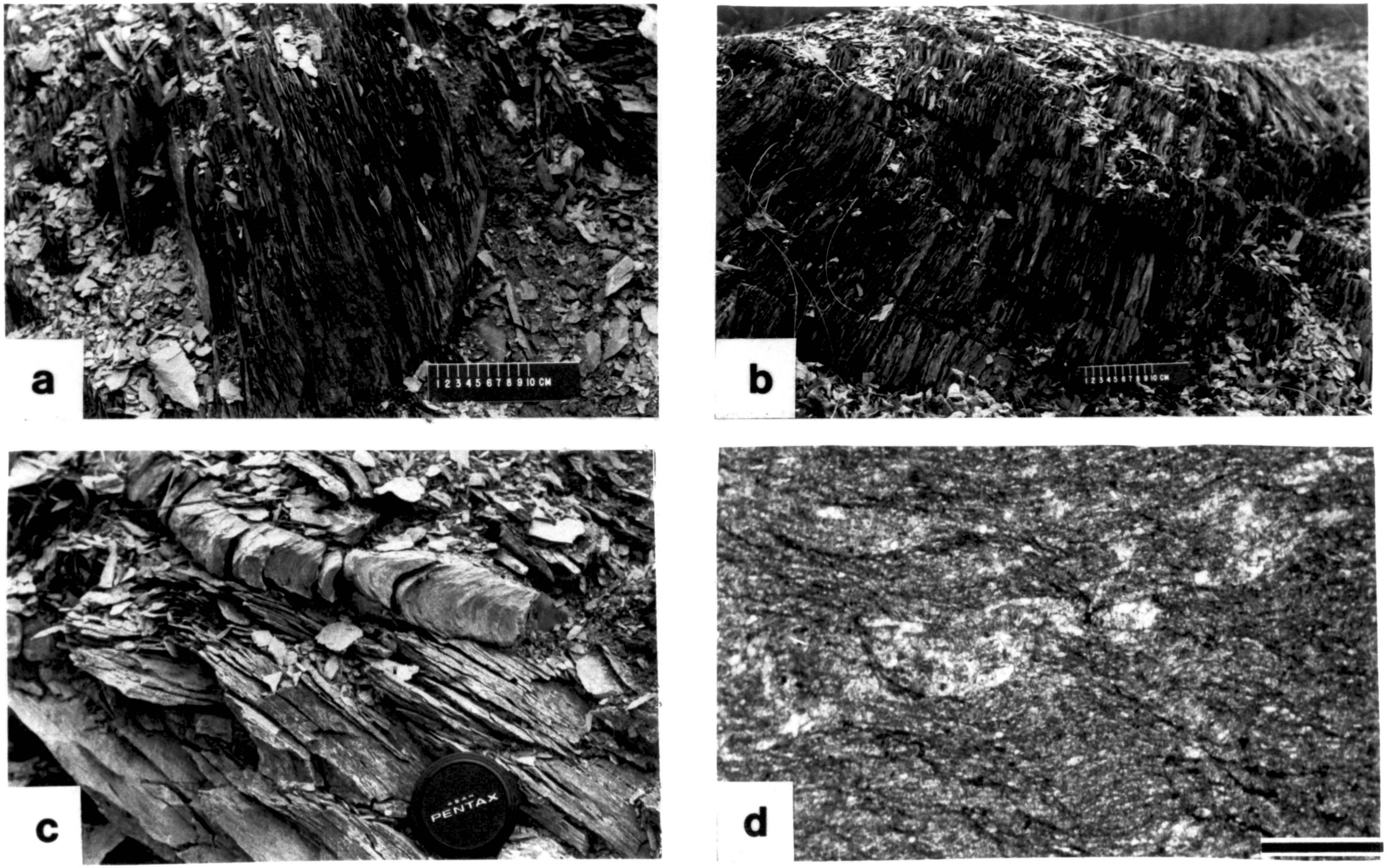

17a

Figure 7. NW-trending S_2 cleavage in the Moccasin and Rich Valley Formations.: a) Mesoscopic F_2 fold with weakly convergent S_2 cleavage fan, Moccasin Formation. Hammer=38 cm. b) Steeply dipping spaced S_2 cleavage, Rich Valley Formation. c) Refraction of S_2 cleavage and mesoscopic faulting, Rich Valley Formation. Hammer=38 cm. d) Closely spaced (near slaty) S_2 cleavage, Rich Valley Formation.

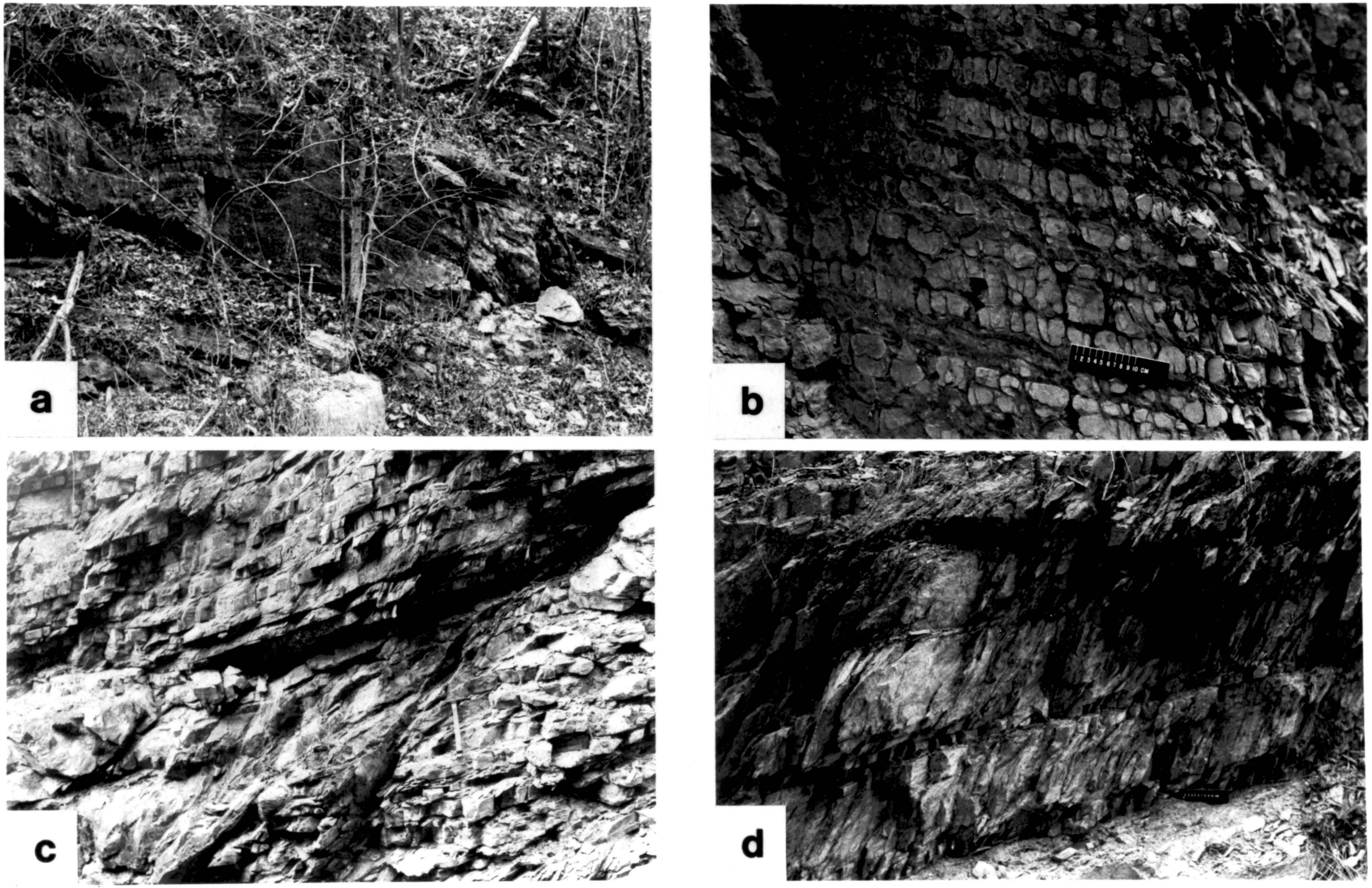
a
b
c
d

S_2 cleavage traces (ave. trend=N70-75°W) are sub-parallel to axial traces of NW-trending mesoscopic F_2 folds but appear to slightly transect sub-regional F_2 fold axes in a counter-clockwise rotational sense (Figure 2 on page 6). Convergent to weakly convergent cleavage fans characteristic of class 1B/1C fold geometry (Ramsay, 1967) are present. Cleavage is commonly refracted across lithologic boundaries and is approximately coplanar and continuous with angular stylolites in adjacent clay-poor limestones. In addition, it is deformed by late-stage extension fractures and is locally kinked. These features indicate that cleavage represents a finite increment of the total rock strain and appears to have behaved in a relatively passive manner during subsequent deformational increments (cf. Alvarez et al., 1976, 1978).

FRACTURES/VEINS

Several sets of calcite-filled fractures (veins) occur in the Ordovician carbonate sequence. The three dominanat vein sets are:

1. Early, somewhat randomly striking, steeply dipping veins typically composed of relatively large (>50u), equant calcite crystals which are heavily twinned. In general these veins occupy planar tensile fractures or conjugate shear sets and are truncated/offset along S_2 cleavage

planes. Ambiguous cross-cutting relations with bedding parallel stylolites are common.

2. NW-trending veins oriented nearly orthogonal to the S_2 cleavage and perpendicular to the principal extension direction (see 'Strain'). The veins are composed of either relatively straight fibrous crystals of calcite or small blocky calcite aggregates and display ambiguous cross-cutting relations with the S_2 cleavage.

3. NE-striking, steeply dipping fractures which post-date the S_2 cleavage. This fracture set cross-cuts the S_2 cleavage and is not ubiquitously mineralized with calcite.

The mineralogy of all veins is identical to that of the carbonate host suggesting a local derivation of vein species during deformation (Beach, 1974, 1977, Kerrich, et al., 1978). Mineral redistribution occurred through pressure solution-transfer processes driven by stress gradients. The morphology of the vein-filling crystals may have been dictated by the rate of fracture dialations.

The randomly striking veins are well developed in the more competent carbonate units and originated prior to the NW-trending S_2 cleavage. Ambiguous cross-cutting relations with bedding-parallel stylolites are indicative of coeval origin. Dilation associated with the NE-trending veins is not recorded by pressure fringes. These veins appear to be early tectonic features which predate the development of the NW-trending cleavage. This stage of veining was probably driven by overburden pressure. NW-trending, gently SW-dipping veins are best developed in well cleaved units and are syntectonic with S_2 cleavage (cf. Beach and Jack, 1982; Winsor, 1983). Where crystals are fibrous, they are relatively straight, indicating nearly coaxial dilation. The post-S_2 NE-trending fractures appear to represent a component of late stage sub-horizontal NW-SE extension.

KINKS AND MICRO-FOLDS

Kink bands and micro-folds of the NE-trending cleavage (S_1) occur near the base of the Rich Valley Formation in the axial portion of the Walker Mountain Syncline (Fig. 6b and 6c). These structures commonly develop in materials with a well defined, pre-existing planar anisotropy (e.g. cleavage) (Cobbold et al., 1971).

NE-trending kink bands are developed in strongly cleaved calcareous shales adjacent to frontal imbricates of the Pulaski-Walker Mountain thrust (Figure 2). They appear as sharp, angular deflections in the S_1 cleavage and commonly have discontinuous to arcuate hinge lines. Micro-folding of the NE-trending S_1 cleavage(Fig. 6c) occurs in the hinge region of the regional F_1 fold. Micro-folds are tight, NE-trending sinusoidal folds and display a weak, stylolitic axial plane cleavage which cross-cuts the S_1 fabric when viewed in thin section (Fig. 6d). Late stage calcite veins occur along fold limbs where the S_1 cleavage has been rotated to form a plane of weakness.

Broad, NE-trending monoclinic F_3 flexures of the spaced cleavage (S_2) occur and resemble large-scale kink bands with less angular hinge areas. The geometry and magnitude of these flexures appear to be dependent on the type and spacing of the cleavage, and on the orientation of cleavage with respect to the local stress field.

The kinks and micro-folds in the hinge area of the syncline appear to be the result of the superposition of nearly coaxial deformational movements. These may be related to regional fold development followed by imbrication of the Pulaski footwall ramp (cf. Schultz, 1983). The F_3 monoclinic flexures of the NW-trending cleavage (S_2) are due to noncoaxial movements post-S_2 development, associated with the emplacement of the Saltville thrust sheet.

MICROSTRUCTURE

"Solution cleavage" (Alveraz et al., 1976, 1978) is well developed in the Middle Ordovician Rich Valley and Moccasin Formations. The NW-trending S_2 cleavage ranges from a closely spaced, near slaty form in calcareous mudrock to a compound tectonic fabric (Gray, 1981) in argillaceous limestone. The compound fabric is characterized by the presence of two approximately coplanar cleavage anisotropies, with a penetrative domainal microfabric preserved in the lithons of a more widely spaced, smooth stylolitic type. The NE-trending S_1 fabric is microstructurally similar to the domainal microfabric of the compound fabric and will not be discussed separately.

CLEAVAGE MICROFABRIC

In both formations a domainal microfabric appears to be transitional with a mesoscopic spaced disjunctive cleavage (Powell, 1979). The domainal microfabric, developed in calcareous mudrock and argillaceous limestone, is defined by sub-parallel, discontinuous-continuous, wispy, clay-rich folia (1-10µ wide) alternating with thicker intercleavage domains (15-40µ wide) where lithologic layering is commonly preserved. (Figure 8). The more widely spaced (0.5-3 cm) disjunctive cleavage in argillaceous limestone is defined by thick (<5 mm) sub-parallel, curviplanar clay partings (Fig. 8b and c). The discrete, rough to smooth folia of the domainal microfabric appear to coalesce into anastomosing, reticulate networks which define the spaced cleavage in outcrop. Cleavage mineralogy is similar to that of the carbonate host with dominantly grain-shape changes and mineralogic redistribution resulting in differentiated zones. Cleavage domains are defined by concentrations of phyllosilicates with moderate to strong dimensional preferred orientation sub-parallel to seam boundaries. Phyllosilicates are generally undeformed, but locally display internal deformation and folding where they abut against more rigid grains (cf. Woodland, 1982). Calcite grains are generally untwinned and greatly depleted in cleavage zones. Adjacent to seams, grains are characterized by a reduction in area, increased aspect ratio and corroded grain boundaries (cf. Gray, 1981). Detrital quartz grains are somewhat concentrated along cleavage folia. Adjacent to folia, grains are weakly elongate and exhibit slightly corroded boundaries while grains between seams are relatively equant with smooth boundaries. Framboidal pyrite is disseminated through the cleavage zones and microlithons, frequently concentrated along cleavage. It occurs as isolated spherules (1-7µin diameter), subspherical to irregularly shaped granular aggregates (<150μin diameter), and disrupted, pseudo-tabular forms which appear to have been rotated from the plane of bedding (Fig. 9d). Calcite, quartz, and phyllosilicates occur in pressure fringes adjacent to pyrite.

PHYLLOSILICATE MINERALOGY

Phyllosilicate minerals are concentrated along cleavage folia and are dimensionally oriented sub-parallel to seam boundaries. Mineralogy of the spacaed cleavage was determined by X-ray diffractometry (Appendix II) to evaluate mineralogic changes accompanying CLEAVAGE DEVELOPMENT. The clay fraction (<2μ population) comprises 10-15 percent of the bulk rock mineralogy and consists dominantly of illite (phengitic mica) and chlorite (partially weathered to vermiculite), plus or minus kaolinite. Illite and chlorite occur as discrete and interstratified phases. In addition to phyllosilicates, the host mineralogy includes calcite (<90%), detrital quartz (<5%) and feldspar (trace).

The crystallinity of illite, reflected by the morphology of the first-order (10A) X-ray peak, has been used to describe the state of diagenetic and metamorphic evolution of low-grade rocks (Frey, 1970, Siddans, 1977, Hoffman and Hower, 1979, Kisch, 1980, Pique, 1982; see Dunoyer de Segonzac, 1970 for review). Sharpening of the 10A peak and an increase in $I_{(002)}/I_{(001)}$ ratio (related to Al/Fe+Mg) re-

Figure 8. Photomicrographs of the S_2 cleavage, Rich Valley Formation.: a) Well developed domainal microfabric (sub-vertical) and folded/ pressure solved vein (sub-horizontal). Bar scale=150μ. b) Domainal microfabric and incipient spaced cleavage, argillaceous limestone. Bar scale=150μ. c) Spaced disjunctive cleavage and late- stage fibrous calcite veins which record extension approximately perpendicular to cleavage. Bar scale=1.0 mm. d) Lateral bifurcation of cleavage folia in the tip region of the spaced S_2 cleavage. Bar scale=150μ.

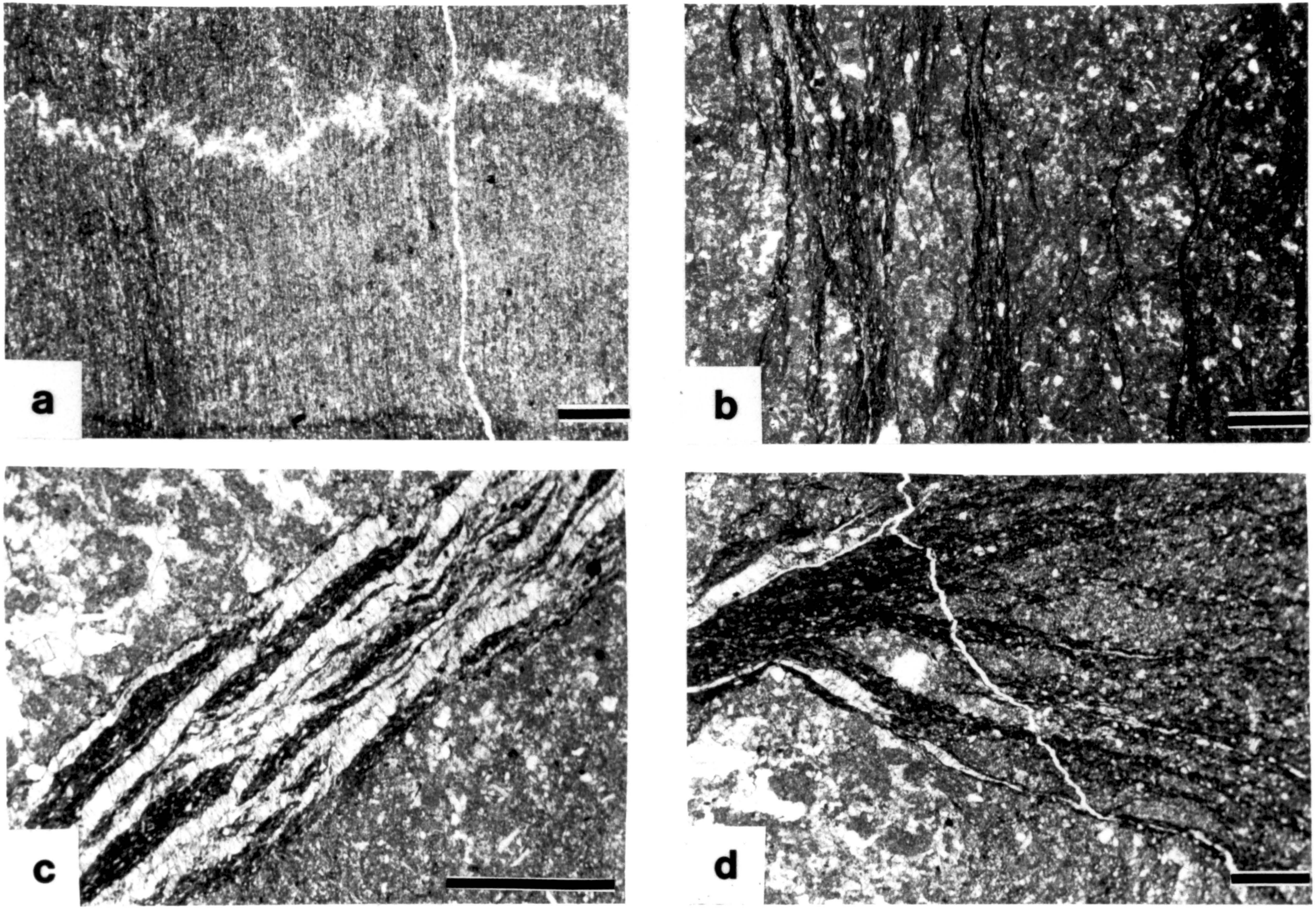
a
b
c
d

flects the chemical and crystallographic evolution of detrital illite to metamorphic white mica (Weaver, 1960, 1961, Kubler, 1964, 1968, Weber, 1972).

Conodont color alteration Indices (Harris et al., 1978) reveal maximum paleotemperatures reached during deformation were 200-300°C. Illite crystallinity and composition varies in the study area, but generally indicates a well crystallized, phengitic white mica (Brindley and Brown, 1980). Assuming little temperature variation, differences appear to be directly related to the intensity of deformation, with higher crystallinities and $I_{(002)}/I_{(001)}$ ratios corresponding to areas of well developed cleavage. Peak widths range from 0.39-0.80 DEGREES 2θ and are in between those characteristic of illites (0.6-1.0 DEGREES 2θ) and well crystallized muscovite (0.20 degrees 2θ) (Brindley and Brown, 1981). The I002/I001 ratio ranges from 0.334 to 0.418, characteristic of phengitic mica (Dunoyer de Segonzac, 1970).

STRAIN

PRESSURE FRINGES

Syntectonic fibrous crystals in pressure fringes (Spry, 1969) have been used to calculate finite strains and incremental strain histories of deformed rocks (Elliot, 1972, Durney and Ramsay, 1973, Wickham, 1973, Wickham and Anthony, 1977, Gray and Durney, 1979). Fringe development is due to inhomogenous stress distribution around rigid inclusions during ductile extension (Selkman, 1983) and records penetrative strain.

Pressure fringes adjacent to pre-tectonic framboidal pyrite aggregates (Love, 1957) in the micritic Rich Valley Formation (Figure 9) consist of nearly straight fibers of calcite, quartz, white mica and chlorite, in that order of abundance. The fibers are generally parallel and undeformed displaying antitaxial growth characteristics (cf. Durney and Ramsay, 1973). The proportion of quartz in fringes is much greater directly adjacent to the framboids (i.e. late in the deformational history) and may indicate a change in the relative solubilities of calcite and quartz as deformation progressed. Cleavage is approximately concordant with fringe boundaries. The penetrative strain recorded by fiber growth is assumed to be comparable in magnitude to that required to form the cleavage.

STRAIN MEASUREMENT

Relatively straight fibers developed adjacent to sub-spherical framboids indicate essentially irrotational, coaxial strain. Measurements were restricted to fringes on near spherical framboids (20-100µIN DIAMETER) AS MORE IRREG-ULARLY SHAPED PYRITES DISPLAY EVIDENCE OF rigid body rotation (e.g. asymmetric fringes). Fiber growth is assumed to be parallel to the principal extension direction in the rock (X) with cleavage approximating the XY principal plane of finite strain (principal axes X>Y>Z; $X=1+e_1$, $Y=1+e_2$, $Z=1+e_3$). Based on the previous assumptions, fringes were examined in three mutually perpendicular sections corresponding to the XY, XZ, YZ principal planes of finite strain. Values of principal extension (e_1) were calculated using a slightly modified version of Durney and Ramsay's (1973) "pyrite method." For straight fibers the equation is:

$$e_1 = L_n/L_o = \text{fringe length/pyrite radius}$$

(cf. Reks and Gray, 1982).

The morphology of fringes in XY and YZ sections infers no substantial change in length parallel to Y (i.e. $1+e_2=1$).

Figure 9. Photomicrographs of pressure fringes adjacent to framboidal pyrite in the Rich Valley Formation (approximate XZ sections).: a) Re-crystallized pressure fringe adjacent to sub-spherical pyrite. Traces of discrete rough to smooth S_2 cleavage folia of the domainal microfabric are sub-vertical. Bar scale=100μ. Note slight pressure solution cannibalism of the fringe by cleavage folia along its left margin (X=2.22). b) Fibrous pressure fringe in moderately cleaved argillaceous limestone. (X=2.0). Bar scale=100μ. c) Fibrous pressure in weakly cleaved argillaceous limestone. (X=1.50). Bar scale=50μ. d) Disrupted pyrite body with well developed pressure fringe. Bar scale=100μ.

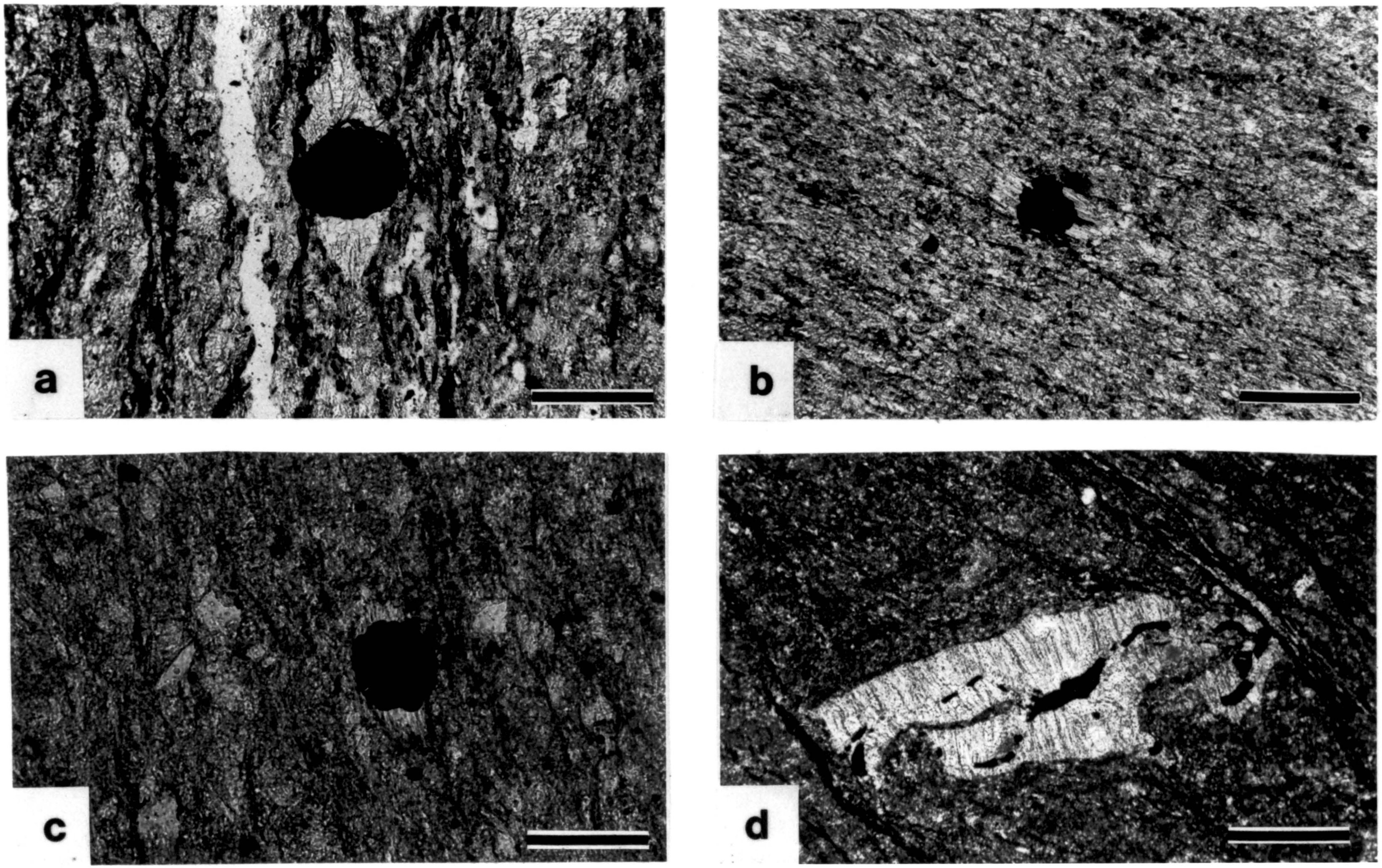
a
b
c
d

No direct measurement of Z can be obtained from fringes but assuming plane strain, $1+e_3 = 1/1+e_1$.

Values of pressure solution shortening (e_3) were estimated along traverses perpendicular to cleavage. The folia are assumed to have formed solely as a result of passive concentration of clays due to pressure solution removal of calcite +/- quartz along the developing seams. Shortening values (e_3) are calculated using the following equation:

$$e_3 = (L - L_o)/L_o$$

where L=traverse length and L_o=pre-deformation length. Length prior to deformation is calculated as follows:

$$L_o = L_m + L_f/F$$

where L_m=cumulative microlithon width, L_f=cumulative folia width, and F=concentration of insolubles (Yontice, 1983). Shortening values determined by the solution method are comparable to, but consistently lower than those determined from pressure fringes (Table 1). Values of pressure solution shortening are subject to uncertainty due to heterogeneous folia development and phyllosilicate recrystallization during deformation. These factors affect the values of L_m, L_f and F and generally tend to reduce the calculated values of shortening. In addition, incipient folia are difficult to detect and accurately measure. This also tends to reduce the value of shortening.

TABLE 1

Comparative Strain Data

Sample	Shortening Values (%) Solution Method	Pyrite Method
RV-03	41.1	55.1
RV-107	44.8	54.9
RV-149	33.6	53.2
RV-194	43.7	55.1
RV-242	18.1	26.0
RV-331	39.1	53.4

Pressure fringes record ductile extension in the matrix and may be a measure of controlled particulate flow (cf. Boradaille, 1979, 1981). However, fringe development may not represent the bulk rock strain. In the study area shortening values determined from pressure fringes are similar to those determined for pressure solution (the dominant cleavage-forming process). This supports the assumption that the strain recorded by pressure fringes approximates that responsible for cleavage development. In this particular case the strain values are comparable, but it is essential to determine the way in which strain partitions during deformation.

STRAIN VARIATION

Fringes occur exclusively in calcareous mudrock of the Rich Valley Formation and are associated with both the NE-trending S_1 and NW-trending S_2 cleavages. Strain calculations assume plane strain with no volume change. Important strain characteristics associated with each cleavage are discussed below.

1) The NE-trending S_1 cleavage is preferentially developed adjacent to the decollement near the base of the Rich Valley Formation in the axial region of the F_1 Walker Mountain syncline. Fibers are straight to curved indicating a component of non-coaxial strain during S_1 development. When curved, the late increments of extension (recorded by fibers closer to the pyrite) are more nearly parallel to S_1 traces. Values of penetrative strain (X Y Z) are generally greater than those associated with S_2 development, ranging from 2.08:1.0:0.48 to 2.56:1.0:0.39 (Appendix I). The NE-trending cleavage is commonly deformed (Figure 8). Thus some fiber curvature may be the result of deformation rather than non-coaxial increments of strain. Incremental strain analysis

of curved fibers was not attempted because of polydeformation.

2) The NW-trending S_2 compound fabric occurs throughout the study area in the Rich Valley and Moccasin Formations. Fibers associated with the S_2 cleavage are relatively straight and undeformed indicating nearly coaxial increments of strain. Values of penetrative strain (X Y Z) are variable, ranging from 1.36:1.0:0.74 to 2.23:1.0:0.45 (Appendix I).

The magnitude of penetrative strain associated with both fabrics is heterogeneous. Variations in grain-scale strain are recorded by adjacent fringes within a single thin section. Standard deviations associated with the mean strain (X) range from 0.12 to 0.34 and depict the heterogeneity of strain at the grain-scale. In general, fringes on FRAMBOIDS SMALLER THAN 20µ IN DIAMETER yield greater than average strains while fringes on framboids greater THAN 100µ IN DIAMETER YIELD LESS THAN AVERAGE STRAINS WITHIN THE SAME thin section (Appendix I). This may be the result of readjustment of the micritic matrix during ductile extension (cf. Beutner and Diegel, in press). When calculating means and standard deviations, only those fringes on pyrites between 20 AND 100µ IN DIAMETER WERE USED.

Penetrative finite strain associated with the development of the S_2 cleavage is heterogeneous on a regional scale with a general decrease in magnitude in a SW to NE direction

(Figure 10). A direct correlation exists between the intensity of fabric development and the grain-scale strain recorded by the fringes. However, the degree of fabric development and the magnitude of strain are independent of position with respect to mesoscopic D_2 structures (cf. Spears, 1983). Integration of finite strain (Hossack, 1978) determined in the Rich Valley Formation indicates a regional or average shortening of 45.3% (Figure 11). The strain trajectory was constructed approximately perpendicular to S_2 cleavage traces (i.e. parallel to the Y-axes of a series of finite strain ellipses).

Open F_2 buckle folds affect nearly all units in the study area. Geometrical relations between the S_2 cleavage and F_2 folds indicate that buckling passively rotated the cleavage into convergent fans about the folds and was a late-stage event associated with cross-structural development. Buckle shortening was calculated by comparing the deformed length of beds with the original (undeformed) length. Values of buckle shortening are low ranging from 5.7% (interlimb angle=155°) to 13.2% (I.L.A.=120°). Slight transection of S_2 cleavage traces by sub-regional F_2 fold axes indicates hinge migration and may represent a late rotational component of strain not recorded by pressure fringes.

Figure 10. Map showing regional strain variation in the Middle Ordovician Rich Valley Formation in the study area.: Values represent Y/Z axial ratios of the penetrative strain ellipsoid determined from pressure fringes. Open ellipses=strain associated with S_1; closed ellipses=strain associated with S_2. Trajectory along which strain was integrated is shown (A-B-C).

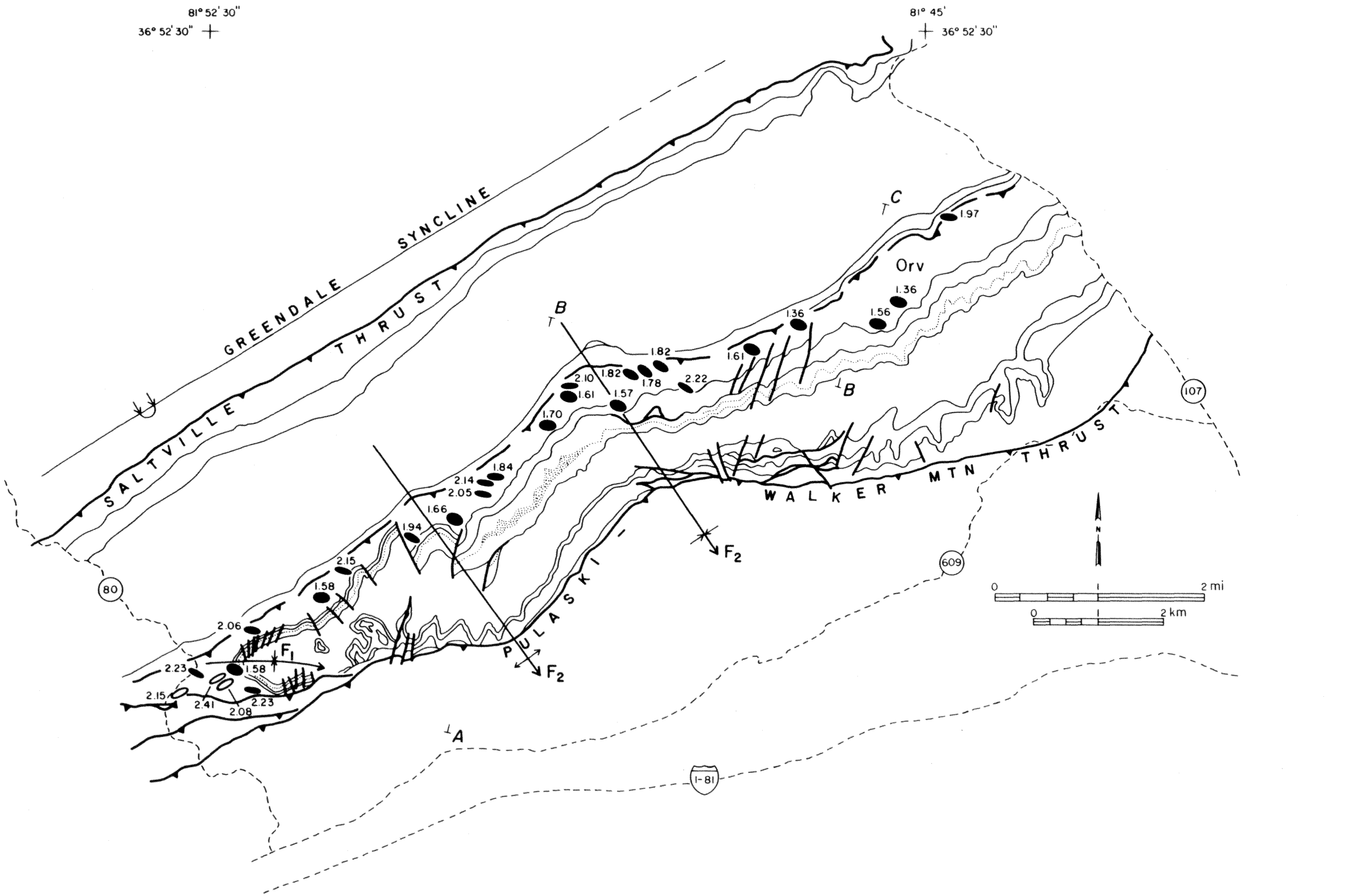
81° 52' 30"
36° 52' 30"
81° 45'
36° 52' 30"
GREENDALE SYNCLINE
SALTVILLE THRUST
WALKER MTN THRUST
PULASKI
Orv
C
B
A
F1
F2
F2
1.97
1.36
1.56
1.36
1.61
1.82
1.82
1.78
2.22
2.10
1.61
1.57
1.70
1.84
2.14
2.05
1.66
1.94
2.15
1.58
2.06
2.23
1.58
2.15
2.41
2.08
2.23
80
609
107
I-81
N
0
2 mi
0
2 km

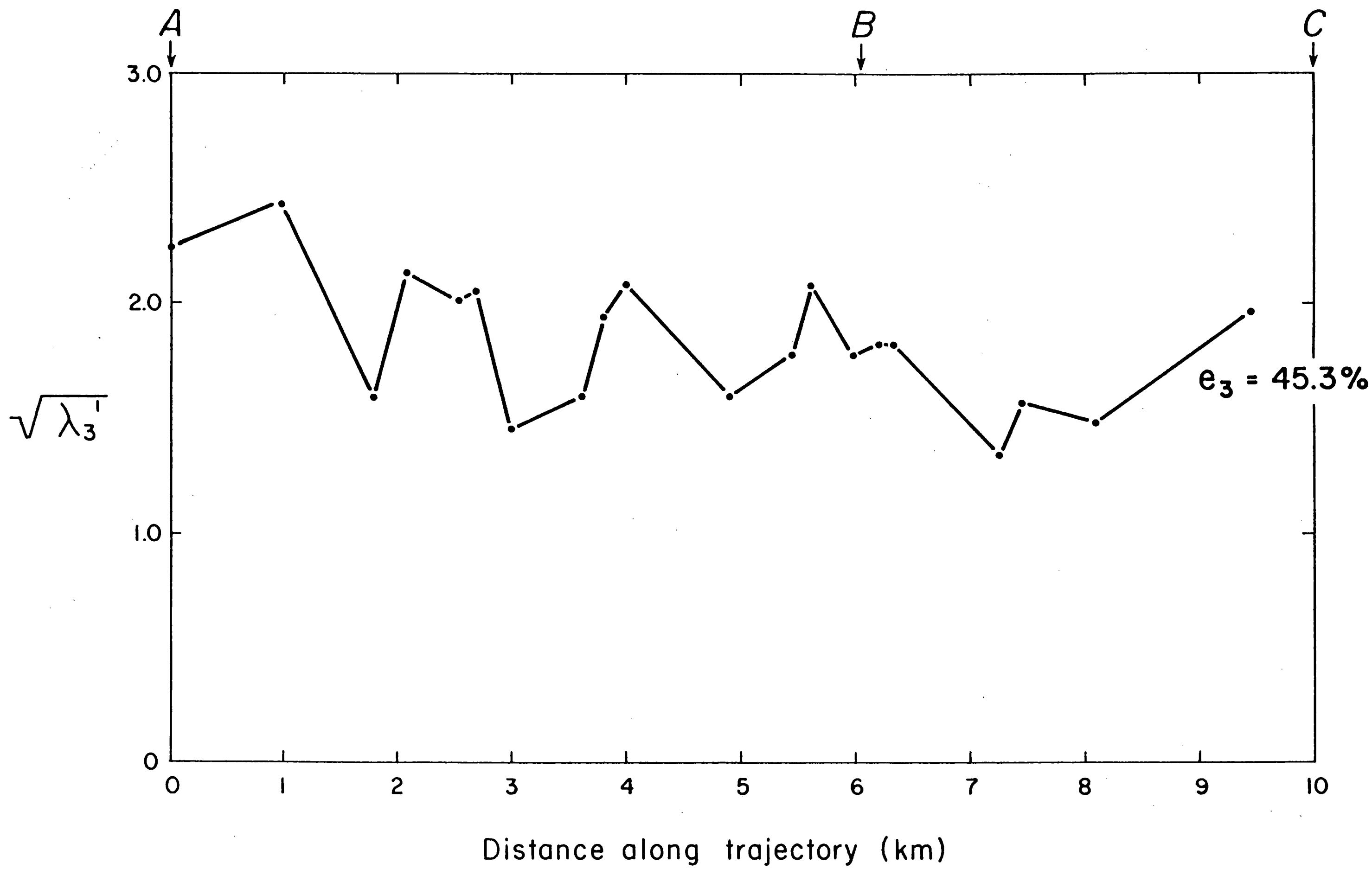

Figure 11. Graph of strain integration along trajectory A-B-C.: Graph of reciprocal quadratic elongation ($\sqrt{\lambda_3}$) versus distance along the trajectory.

DISCUSSION

DEFORMATION MECHANISMS

Several deformation mechanisms contributed to the total (bulk rock) strain. The deformation mechanisms were lithologically dependent with pressure solution accompanied by controlled particulate flow dominant in the fine-grained, somewhat argillaceous carbonates and intracrystalline, plastic deformation dominant in the more competent, relatively clay-poor lithologies (i.e. medium- to massively bedded carbonates). Sub-greenschist prograde mineral reactions involving the aggradation of detrital/diagenetic phyllosilicates were responsible for the final cleavage mineralogy.

Microfabric analysis indicates that cleavage folia are pressure solution surfaces (cf. Reks and Gray, 1982). Evidence for pressure solution includes: concentration of clay minerals along folia, truncation and/or offset of fossil fragments, sparry calcite-filled fenestrae and pre- to syntectonic calcite veins along folia despite a lack of cataclastic texture. Dilational pressure fringe zones in conjunction with the lack of intracrystalline matrix deformation indicate dissolution and transfer of mobile species was accompanied by controlled particulate flow in the micritic matrix (cf. Borradaille, 1979, 1981). The bulk rock ductile extension may have initiated folia which subsequently became solution surfaces. Loss of support due to dissolution of calcite and quartz grains may have allowed passive mechanical rotation of phyllosilicates, thus contributing to the dimensional preferred orientation. Deformation twinning of sparry calcite in pre-S_2 veins indicates a component of intracrystalline strain in mechanically more rigid material.

Syndeformational changes in illite crystallinity and chemistry indicate sub-greenschist metamorphic mineral reactions occurred concurrently with pressure solution processes. Phyllosilicate mineralogy of the spaced cleavage evolved through prograde metamorphic mineral reactions which involved the aggradation of diagenetic clay minerals to well crystallized micas and chlorites. The progressive reaction proposed to explain the phyllosilicate assemblage of the spaced cleavage is:

$$\text{illite/montmorillonite} \rightarrow \text{phengitic mica} + \text{chlorite}$$

(probably via a mixed illite/chlorite interstratified phase) (Weaver et al., 1971; Velde, 1977; Gray, 1981). The reactions are dependent on the composition of the aqueous phase, and generally buffer pH to values above neutrality (Beach, 1979). In the 200-250°C temperature range the solubility of silica is maximized at pH>8.5. Therefore, as metamorphic reactions progess during deformation, the relative solubilities of mineral species may vary (e.g. calcite and quartz).

Pressure solution (accompanied by controlled particulate flow) in response to non-hydrostatic stress gradients appears to have been the dominant cleavage-forming process. Mineralogic differentiation and the development of preferred orientation resulted from the redistribution of calcite and quartz, and passive mechanical rotation and recrystallization of phyllosilicates. Entianced diffusion along evolving folia may have localized mineral reactions and pressure solution along these surfaces (cf. White and Knipe, 1978; Wober, 1981; White and Johnson, 1981; Knipe, 1981).

CLEAVAGE EVOLUTION

Cleavage domains are mineralogically differentiated zones depleted in calcite and enriched in strongly aligned phyllosilicates. Cleavage morphology is dependent on lithology and strain state. Sharp contrasts in cleavage attributes occur between lithologies whereas gradational morphologic variations occur in one unit as a function of strain (cf. Simon and Gray, 1982). Solution transfer of calcite and phyllosilicate recrystallization are envisioned to be the dominant cleavage-forming processes (Figure 12).

Figure 12. Evidence of pressure solution associated with the S_2 cleavage, Rich Valley Formation.: a) Thinning and truncation of trilobite fragment along S_2 cleavage (domainal microfabric), argillaceous limestone. Note deflection of cleavage folia adjacent to fossil fragment. Bar scale=1.0 mm. b) Offset of calcite vein and truncation of fossil fragment along S_2 cleavage folia, argillaceous limestone. Bar scale=150μ. c) Close-up of truncated fossil fragment shown in (b). Bar scale=100μ.

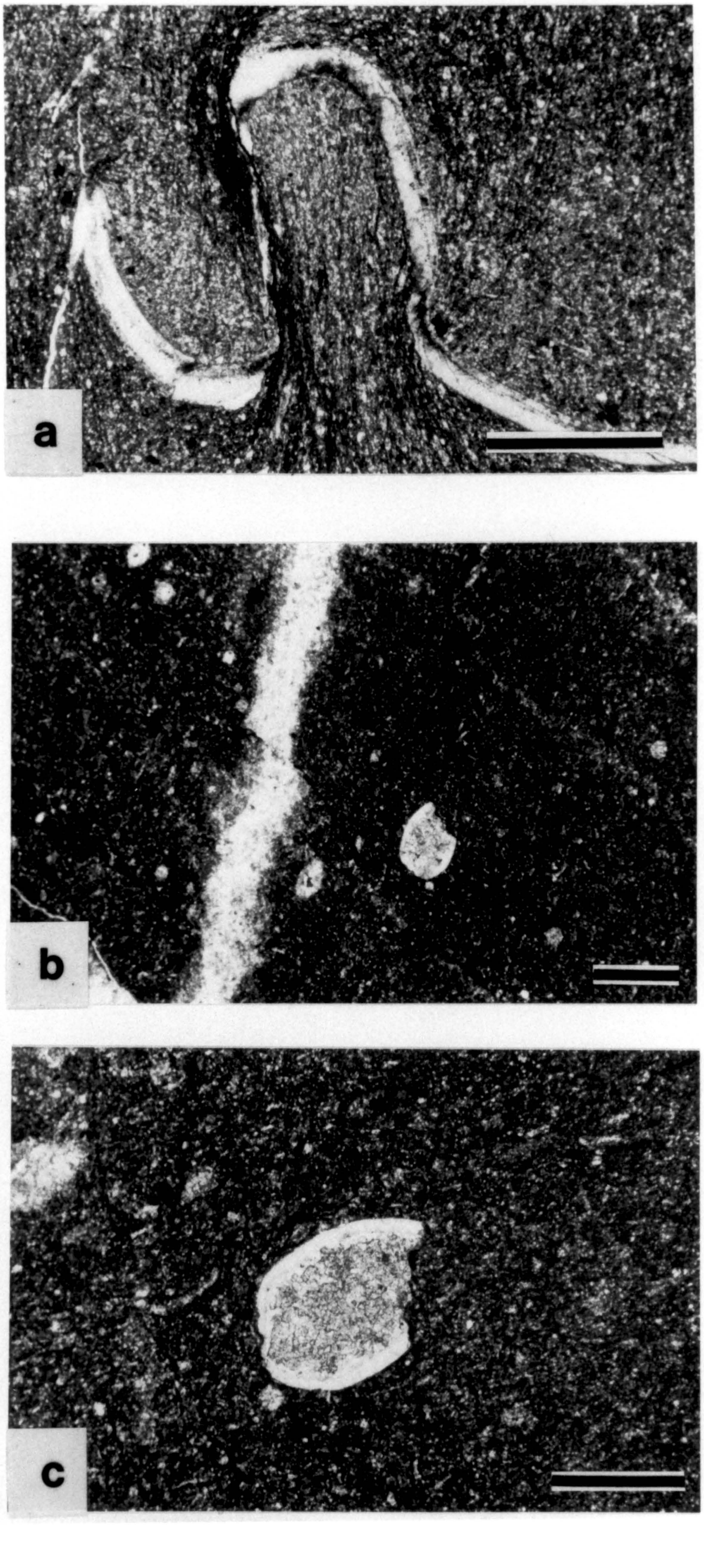
a
b
c

Cleavage evolution appears to be strongly influenced by the percentage and distribution of clay in the host fabric (cf. Marshak, 1982, Yonkee, 1983). Folia are thinner, more numerous and more uniformly developed in calcareous mudrock, as opposed to thicker, less numerous and localized in argillaceous limestone. Thus when clay is relatively abundant, discrete, wispy-continuous, anastomosing networks of folia develop during progressive deformation. When clay is sparse in the host fabric, preferential enhancement of discrete folia of the domainal microfabric is favored, resulting in thicker, more widely spaced cleavage planes. The developing seams of the spaced cleavage tend to collapse the intervening wedges or lenses of rock by extending solution surfaces in the tip region of folia (Fig. 8d) (cf. Fletcher and Pollard, 1982). The dominant morphological difference between the two cleavage fabrics is mainly the scale of the cleavage domains. The relative timing of cleavage formation with respect to metamorphic reactions involving phyllosilicate minerals may also influence final cleavage morphology.

Heterogeneous spatial development of cleavage is common on a microscopic scale and reflects variations in the magnitude and location of strain during deformation. Folia are extremely well developed adjacent to relatively rigid objects (e.g. framboidal pyrite, detrital quartz grains, and fossil fragments) and commonly coalesce in the inner arc of hinge regions of micro-buckle folds. These areas of local stress concentration appear to have served as nucleation sites for folia. Increasing strain resulted in the lateral propagation of individual folia and the reduction in amplitude variations of the undulose seams. This tended to increase the continuity of the microfabric and collapse the fabric of the microlithons. Maintenance of shortening also must have exerted control on seam development. Commonly as one seam thins or terminally bifurcates another en echelon seam thickens.

Thus mineralogy and fabric of the parent micrite partly controlled the initiation of folia. Final cleavage morphology is dependent on clay content and distribution, and strain partitioning between different deformation mechanisms.

Cleavage commonly form convergent fans around open F_2 folds, is refracted across lithologic boundaries and is deformed by late stage extension fractures. These features indicate that development of the cleavage anisotropy represented a finite increment of strain early in the deformational history and appears to have acted passively during subsequent increments.

STRAIN DEVELOPMENT

Syntectonic mineral fibers in pressure fringes associated with the NW-trending S_2 cleavage are virtually straight and undeformed in three dimensions. Fibers indicate closely coaxial penetrative strain with sub-vertical extension in the S_2 cleavage plane. There is no microstructural evidence indicating extension or contraction parallel to the Y-direction of the strain ellipsoid, nor is there evidence indicating two successive episodes of penetrative deformation during cross-structural evolution. In thrust zones, compressive strains due to layer parallel shortening are common at the frontal-tip portion of the fault and shear strains at the lateral-tip. A wide range of finite strain ellipsoids may result from the superposition of, or synchronous addition of, two or more strain components (Coward and Potts, 1983, Coward and Kim, 1981).

Differential movement of a thrust sheet may lead to the productin of a regional wrench-type shear capable of producing structures oblique to the direction of tectonic transport. A non-coaxial penetrative strain path should be associated with cross-structures generated in response to such a combination of LONGITUDINAL STRAIN ($\sqrt{\lambda_3}$) and layer normal shear strain (γ_2). Although combinations of layer parallel shortening and layer normal dextral shear, or layer parallel shear and layer normal dextral shear may explain the oblique attitude of the cross-structures (Figure 13) the rotational strain paths associated with such shears are incompatible with strain data from the study area. Lack of evidence for rotation of strain axes during deformation makes it impossible to factor the bulk strain into COMPONENTS OF $\sqrt{\lambda}$, γ_1, γ_2. A nearly coaxial strain history and the nature of the S_2 fabrics (bedding-cleavage angles>80°) are most easily interpreted to be the result of layer parallel shortening (Engelder and Engelder, 1977, Engelder and Geiser, 1979) oblique to the transport direction.

Variable ease of detachment along the evolving Saltville thrust may have led to the propagation of a compressional front (frontal tip-line) oblique to the direction of tectonic transport (Figure 14). The oblique migration of a segment of the frontal tip-line probably resulted from a greater degree of decollement thrusting to the southwest along the evolving Saltville fault. The gradual eastward swing in the cleavage altitude and decrease in strain from southwest to northeast (Figure 2, Figure 10) reflect variations in the orientation and magnitude of longitudinal strain associated with tip-line migration. Slight transection of sub-regional F_2 folds by the earlier formed S_2 cleavage indicates that some hinge migration occurred, possibly in response to a minor component of layer normal dextral shear late in the deformation. In addition, a set of NE-trending, steeply NW-dipping fractures post-date the NW-trending S_2 cleavage.

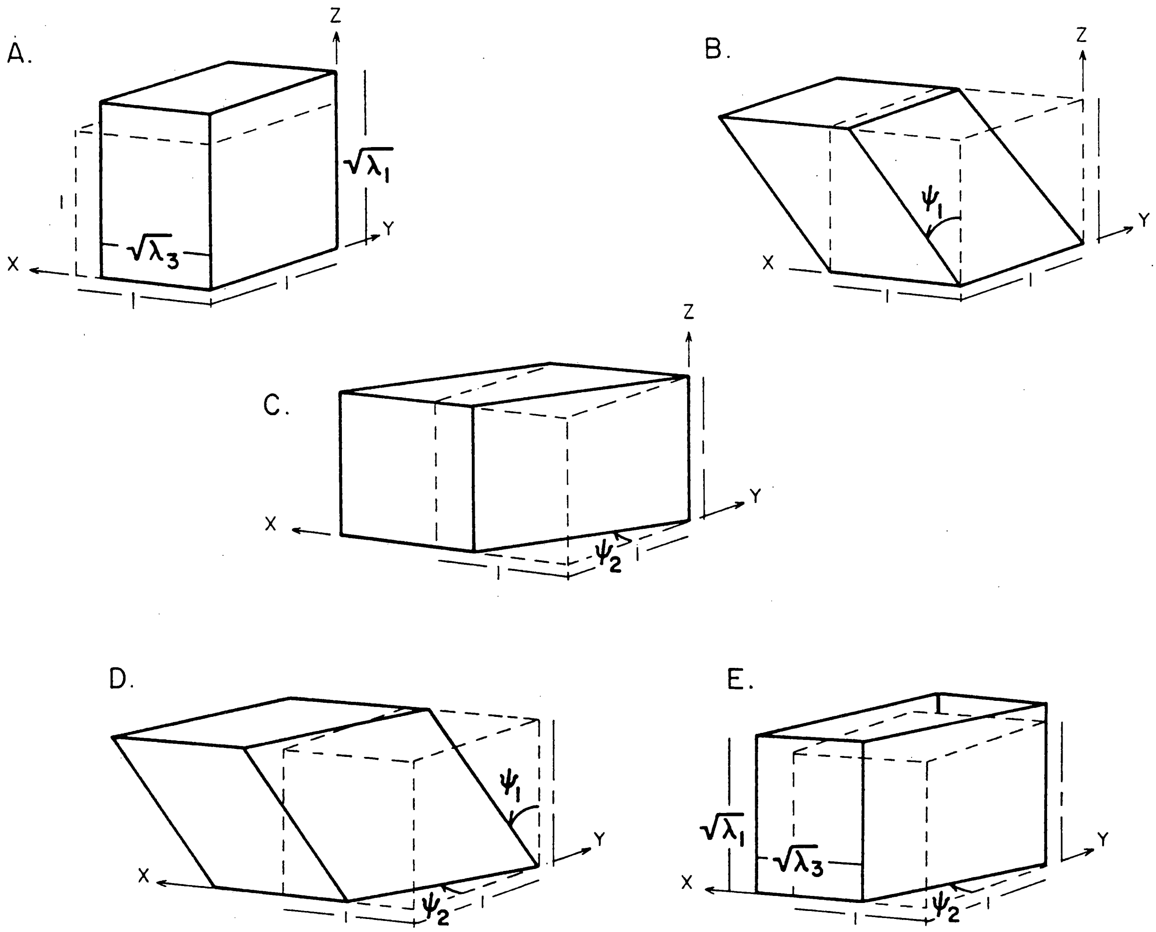

Figure 13. Factorization of three-dimensional strain.: a) Layer parallel shortening. b) Layer parallel shear-due to shear in a thrust system. c) Layer normal shear-due to differential thrust sheet movement. $\sqrt{\lambda_1}=1+e_1$, $\sqrt{\lambda_3}=1+e_3$, $\psi_1=\tan\chi_1$, $\psi_2=\tan\chi_2$. d) Combination of layer parallel shortening and layer normal dextral shear. e) Combination of layer parallel shear and layer normal dextral shear.

The fractures indicate a component of late-stage sub-horizontal extension not recorded by mineral growth in pressure fringes. Late-stage layer normal dextral shear may have been the result of a greater relative contribution of a lateral-tip portion of the Saltville thrust in response to a greater degree of thrusting to the southwest.

DEFORMATION CHRONOLOGY

Interrelations among structural elements, fabric data and geologic map patterns define a distinct structural style in the study area and record the kinematics of regional structural evolution. The general structural chronology is:

1. Walker Mountain Syncline formation and the emplacement of the Pulaski thrust sheet,

2. Cross-structural development deforming the Saltville sheet and the leading edge of the Pulaski sheet, and

3. Final emplacement of the Saltville sheet.

Work by Stanley (1983) indicates that a variety of megascopic footwall structures are commonly developed during the emplacement of the overriding thrust sheet. The map ex-

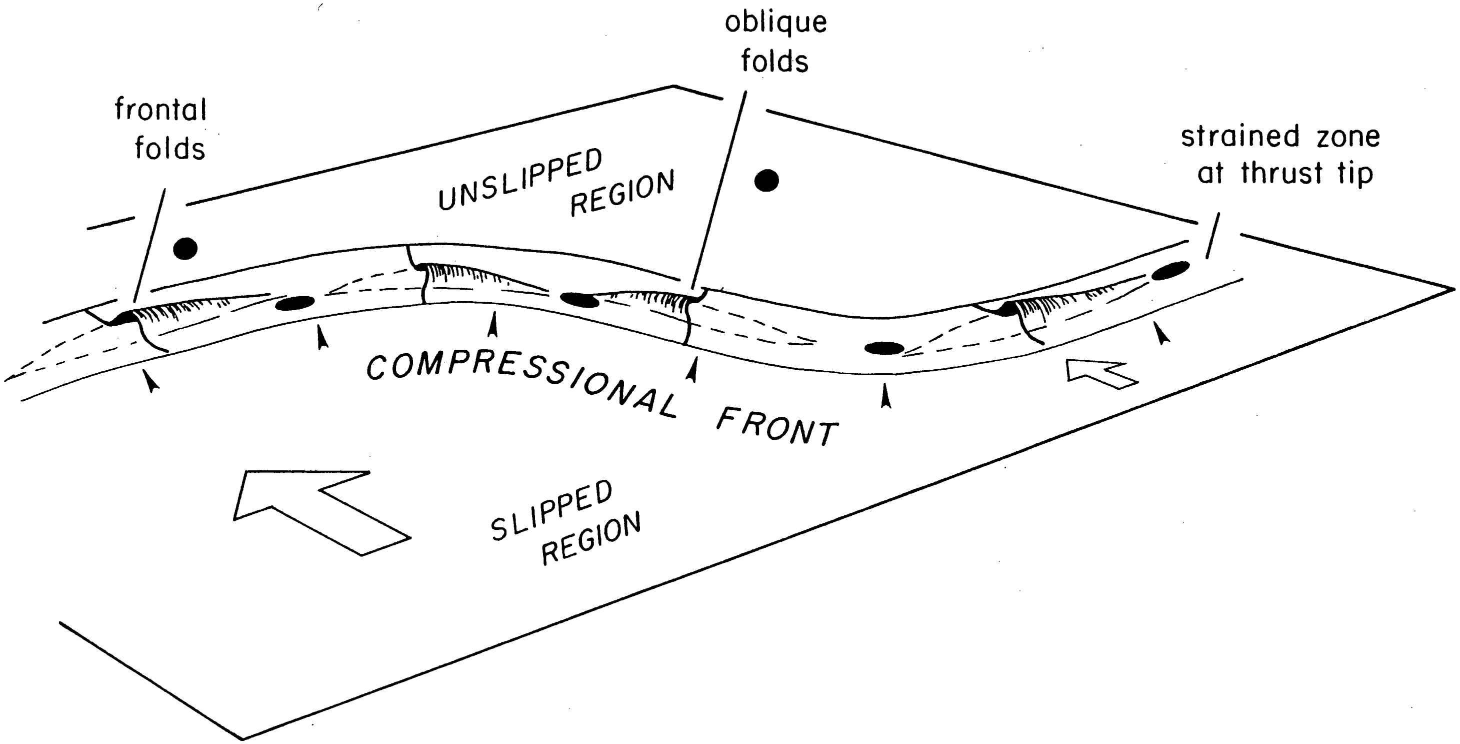

Figure 14. Diagramatic representation of a subhorizontal thrust plane showing the strained tip region undergoing differential displacement. Finite strains associated with tip-line propagation are shown (modified from Coward and Potts, 1983).

pression of these structures is contingent on the erosional level.

At the southwestern termination of Walker Mountain, formations ranging in age from Ordovician to Devonian are involved in regional (F_1) footwall folding (Figure 2, Figure 5). Structural data indicate that evolution of the sub-Pulaski thrust Walker Mountain syncline has not been entirely passive (cf. Stanley, 1983). Detachment between the competent Ordovician Effna/Lenoir Formations and the overlying incompetent Rich Valley Formation is indicated by strong localized mesoscopic deformation adjacent to the contact. Detachment and folding of the overlying Ordovician-Devonia strata are best explained by ramping of the decollement from the Cambrian Rome Formation up-section into the base of the Ordovician Rich Valley Formation (possibly preceded by, or accompanied by active buckle folding) (cf. Bajak, 1983). Ramp-induced folding (Wiltschko, 1978, 1981) was followed by propagation of the Pulaski thrust through part of the pre-existing fold (Figure 15).

Break-thrusting of the Pulaski fault preserved the steeply dipping forelimb of the fold beneath the overriding thrust sheet. Final emplacement of the overlying Pulaski thrust sheet modified the fold and deformed the earlier cleavage. Nearly coaxial micro-folding of the NE-trending S_1 fabric occurs exclusively near the base of the Rich Valley Formation in the axial zone of the Walker Mountain Syncline.

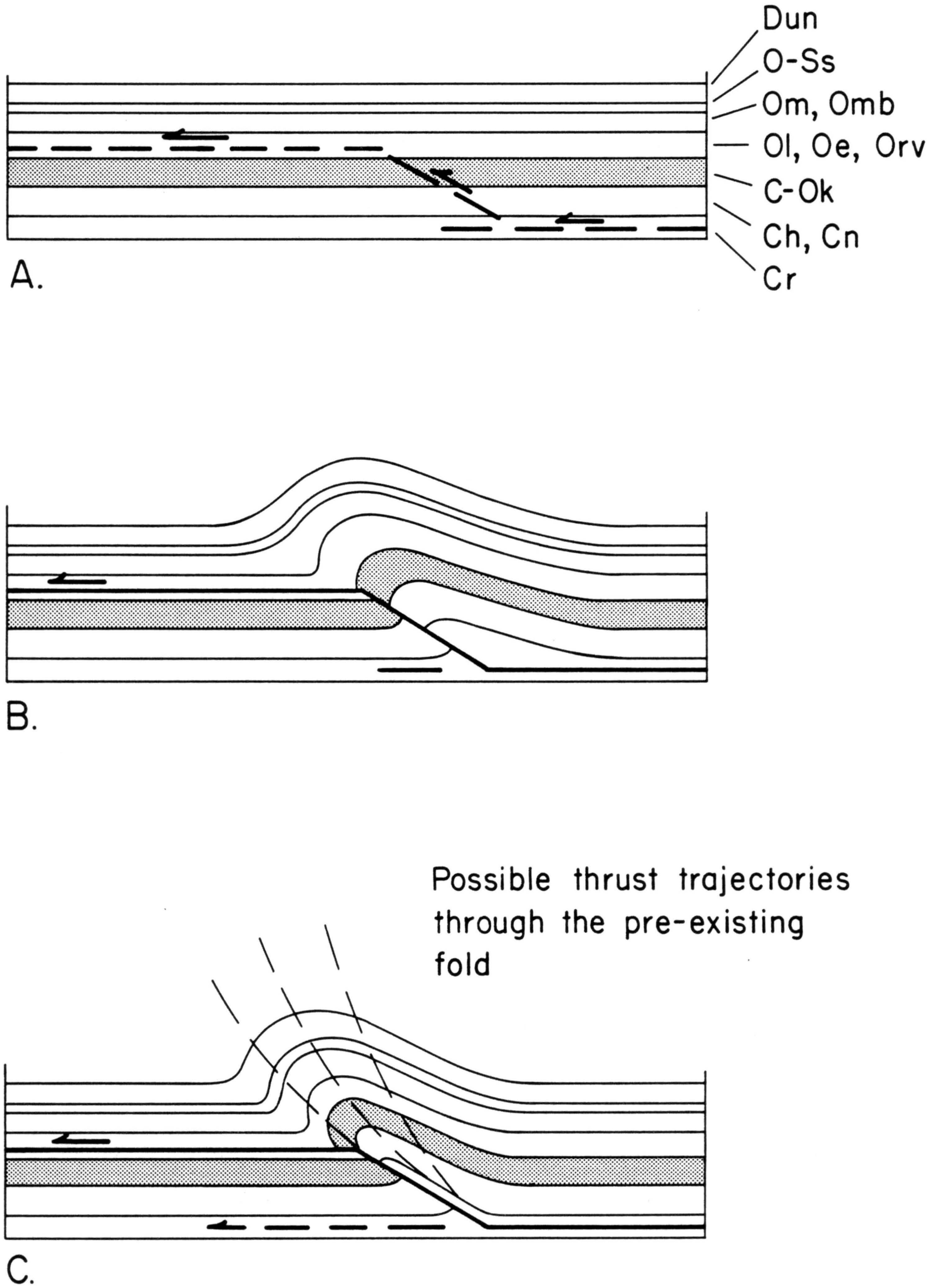

Figure 15. Schematic cross-sections depicting the development of a sub-thrust syncline due to ramp-induced folding followed by break-thrusting through the fold.: a) Thrust trajectory. b) Ramp-induced folding. c) Asymmetric fold developed above a ramp and possible thrust trajectories through the fold (dashed).

The NW-trending cross-structures obliquely overprint a portion of the Saltville sheet and the leading edge of the Pulaski sheet in a continuous 10-15 km zone along strike. Sub-regional cross folds affect the attitude of units in both thrust sheets with a strong spaced cleavage preferentially developed in the Ordovician Rich Valley and Moccasin Formations.

Two approximately coplanar NW-trending cleavage fabrics are developed with their morphology primarily dependent on lithology (see 'Cleavage Microfabric'). Both fabrics trend approximately N70-75 W, form convergent cleavage fans with respect to open NW-trending mesoscopic F_2 folds and are refracted across lithologic boundaries. Sub-regional F_2 fold axes are slightly transected by the earlier formed S_2 cleavage in a clockwise rotational sense. Development of the mesoscopic structures was sequential and fairly continuous. Cleavage was initiated early in the deformational sequence prior to folding and oblique to the overall northwest direction of tectonic transport. NW-trending contraction faults are essentially absent, although reactivation of the detachment near the base of the Rich Valley Formation produced local NW-trending folds.

Timing relations of NE- and NW-trending cross-faults to other structures is problematic. The cross-faults occur exclusively in the Ordovician Rich Valley through Martinsburg sequence and have a consistent right-lateral sense of offset.

These faults do not offset the decollement near the base of the Rich Valley Formation and do not generally affect the attitude of the S_2 cleavage. Cross-faulting probably occurred during regional F_1 folding. Preferential reactivation of suitably oriented faults probably occurred during the development of the NW-trending S_2 cleavage and associated F_2 folds.

The trace of the Walker Mountain-Pulaski thrust is arcuate to irregular while the trace of the Saltville thrust is nearly linear. The F_1 Walker Mountain Syncline is developed in the footwall of the Pulaski thrust and is overprinted by the cross-structures. NW-trending F_2 cross-folds deform units of the Saltville thrust sheet in addition to the leading edge of the Pulaski sheet and appear to have developed in response to decollement thrusting along the Saltville Fault. These observations indicate that ramp-induced folding and subsequent fold modification due to the emplacement of the Pulaski sheet occurred prior to Saltville thrusting. A chart depicting the relative deformation chronology is shown in Figure 16.

Limited evidence for post-S_2 mesoscopic deformation and lack of associated penetrative fabrics imply relatively passive emplacement of the Saltville sheet post cross-structural development. Fairly open NE-trending F_3 kink folds which deform S_2 record the NW-directed movement of the sheet and provide evidence for Saltville thrusting post S_2 development.

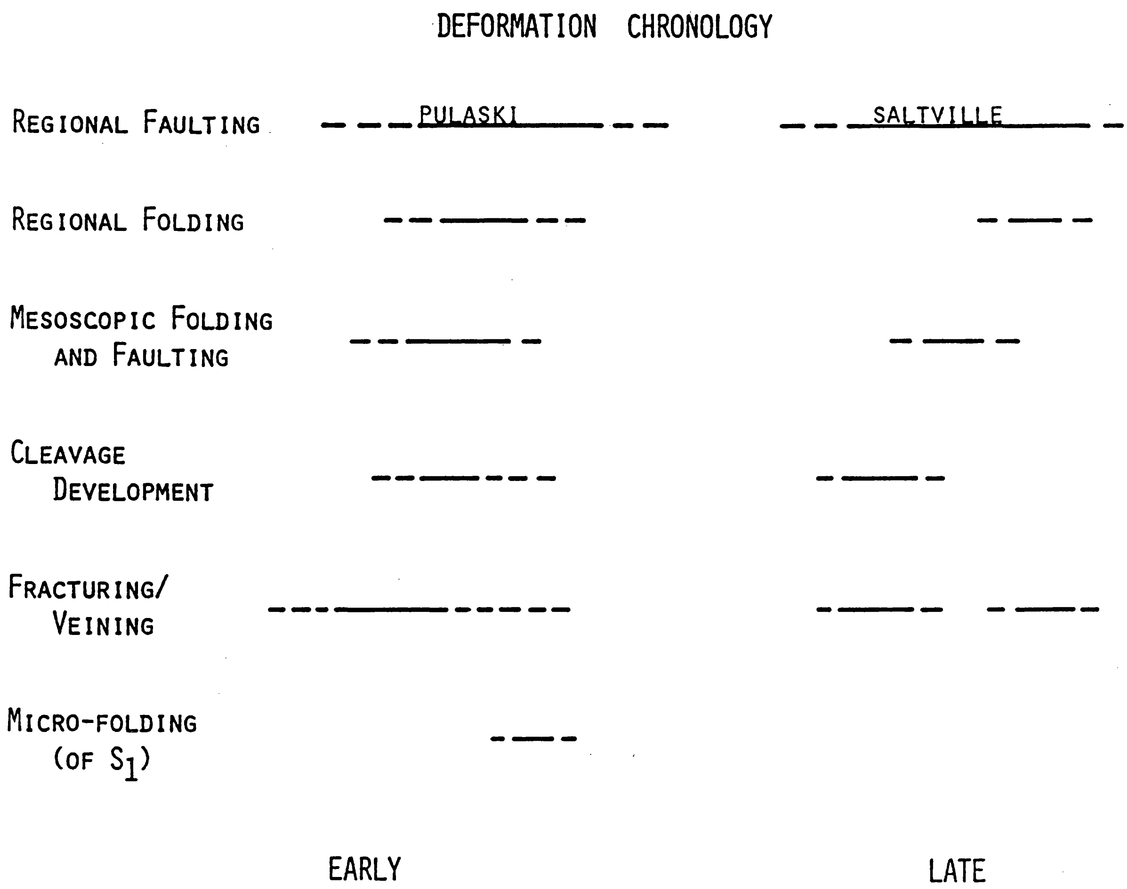

Figure 16. Chart of relative deformation chronology.

CONCLUSIONS

Analysis of mesoscopic structural elements, fabric data and strain data enable the formation of a tectonic model to explain the evolution of cross-structures at the termination of Walker Mountain. In this portion of the southwestern Virginia Valley and Ridge Province, the Saltville thrust sheet and the leading edge of the Pulaski sheet have suffered polyphase Alleghanian deformation due to several pulses of NW-directed thrusting. Deformation was protracted, sequential and generally continuous with the following three distinct phases recognized.

1) Development of the regional NE-trending Walker Mountain Syncline. Asymmetric folding was initiated as the decollement ramped from the Cambrian Rome Formation upsection into the Ordovician Rich Valley Formation. Subsequent fold truncation resulted as the Pulaski thrust propagated through the hinge region of the anticline carrying the southeast limb over the northwest limb. At the present erosional level the Walker Mountain syncline is preserved in the footwall of the Pulaski thrust sheet. A strong but local NE-trending cleavage (S_1) is developed adjacent to the decollement at the base of the Rich Valley Formation. In the axial region of the Walker Mountain Syncline the S_1 cleavage is commonly kinked or refolded in a near coaxial manner. The

numerous NE- and NW-trending transcurrent dextral faults probably developed during this phase of deformation (D_1).

2) Evolution of the NW-trending S_2 cleavage and buckle folds in the Saltville sheet and the leading edge of the Pulaski sheet. The cross-structures developed oblique to the northwest direction of tectonic transport and show no evidence of rotation into their present orientation. They appear to have been superimposed on approximately homoclinally SE-dipping strata that had been previously folded into the Walker Mountain Syncline. There is also no structural evidence for a subsurface NW-trending lateral ramp.

The S_2 cleavage evolved primarily through pressure solution processes associated with approximately coaxial plane strain. Strain data in conjunction with S_2 cleavage characteristics are indicative of layer parallel shortening oblique to the overall direction of tectonic transport. The penetrative strain is best explained by the oblique propagation of a portion of the frontal-tip of the Saltville decollement. The axes of late-stage sub-regional F_2 buckle folds are slightly transected by the earlier formed S_2 cleavage. Hinge migration may have occurred in response to a minor component of layer normal dextral shear late in the deformational sequence.

3) Emplacement of the Saltville thrust sheet in response to NW-directed thrusting. Sporadic open kink folds of the S_2 cleavage and lack of post-S_2 penetrative deforma-

tion imply relatively passive emplacement of the Saltville sheet after cross-structural development.

The polyphase kinematic deformational sequence proposed for the southwestern end of Walker Mountain may be unusual for the Virginia Valley and Ridge Province and directly applicable only to the area studied. On the other hand, studies of this type are not yet abundant and similar structures may yet be found in other areas of the orogen.

Cross-structures deform the Saltville thrust sheet and the leading edge of the Pulaski sheet. This indicates that the Pulaski sheet was emplaced <u>prior to decollement thrusting</u> along the Saltville fault. Structural relations in the study area provide direct evidence of the complex internal strains which may develop in a thrust sheet subject to differential tectonic movements during emplacement.

REFERENCES CITED

Alvarez, W., Engelder, T. and Lowrie, W., 1976. Formation of spaced cleavage and folds in brittle limestone by dissolution. Geology, 4, 698-701.

Alvarez, W., Engelder, T. and Geiser, P. A., 1978. Classification of solution cleavage in pelagic limestones. Geology, 6, 263-266.

Bajak, D., 1983. An investigation of strain patterns and mesoscopic structures associated with ramp-induced folds. Unpubl. M.S. thesis, Virginia Polytechnic Institute and State University, Blacksburg, Virginia, 120 p.

Bartholomew, M. J., 1979. Thrusting component of shortening and a model for thrust fault development at the Central/Southern Appalachian juncture. Geol. Soc. Am. Absts. w/ Progs., 11, 384-385.

Beach, A., 1974. A geochemical investigation of pressure solution and the formation of veins in a deformed greywacke. Contrib. Mineral. Petrol., 46, 61-68.

_____ 1977. Vein arrays, hydraulic fractures and pressure solution structures in a deformed flysch sequence, S. W. England. Tectonophysics, 40, 201-225.

_____ 1979. Pressure solution as a metamorphic process in deformed terrigenous sedimentary rocks. Lithos, 12, 51-58.

_____ 1982. Strain analysis in a cover thrust zone, external French Alps. Tectonophysics, 88, 333-346.

_____ and Jack, S., 1982. Syntectonic vein development in a thrust sheet from the external French Alps. Tectonophysics, 81, 67-84.

Beutner, E. and Diegal, F., in press. Determination of fold kinematics from syntectonic fibers in pressure shadows, Martinsburg slate, New Jersey. Am. J. Sci.

Borradaile, G. J., 1979. Strain study of the Caledonides in the Islay region, S.W. Scotland: implications for strain histories and deformation mechanisms in greenschists. J. Geol. Soc. Lond, 136, 77-88.

_____ 1981. Particulate flow of rock and the formation of cleavage. Tectonophysics, 72, 305-321.

Boyer, S. E. and Elliot, D., 1982. Thrust systems. A.A.P.G. Bull., 66:9, 1196-1230.

Brindley, G. W. and Brown, G. (eds.), 1980. Crystal structures of clay minerals and their X-ray identification. Mineralogical Soc., Lond., 495 p.

Burchfiel, B. C., 1980. Tectonics of foreland fold and thrust belts. In, Exploration Techniques in Foreland Fold and Thrust Belts; A.A.P.G. and R.M.A.G. Short Course.

Butts, C., 1933. Geologic Map of the Appalachian Valley in Virginia with explanatory text. Va. Geol. Survey Bull., 42.

_____ 1940. Geology of the Appalachian Valley in Virginia; Part I. Va. Geol. Survey Bull.,52, 566 p.

_____ and Edmundson, R. S., 1943. Geology of the southwesternend of Walker Mountain, Virginia. Geol. Soc. Am. Bull., 54, 1669-1692.

Calver, J. L., 1963. (Compiler) Geologic map of Virginia. Virginia Division of Mineral Resources, Charlottesville, Virginia.

Cobbold, P. R., Cosgrove, J. W. and Summers, J. M., 1971. Development of internal structures in deformed anisotropic rocks. Tectonophysics, 12:7, 23-53.

Cooper, B. N., 1961. The grand Appalachian excursion. Virginia Polytechnic Institute and State University Engr. Ext. Ser. Gdbk., 1, 187.

Coward, M. P., 1982. Surge zones in the Moine thrust zone of NW Scotland. J. Struct. Geol., 4:3, 247-256.

Coward, M. P. and Kim, J. H., 1981. Strain within thrust sheets. In: K. R. McClay and N. J. Price (eds.), Thrust and Nappe Tectonics. Geol. Soc. Lond. Spec. Publ. 9, 275-292.

_____ and Potts, G. J., 1983. Complex strain patterns developed at the frontal and lateral tips to shear zones and thrust zones. J. Struct. Geol., 5:3/4, 383-399.

Dunoyer de Segonzac, G., 1970. The transformation of clay minerals during diagenesis and low-grade metamorphism: a review. Sedimentology, 15, 281-346.

_____ and Ramsey, J. G., 1973. Incremental strain measured by syntectonic crystal growths. In: A. Kees and R. Scholten (eds.), Gravity and Tectonics. Wiley and Sons, Inc., New York, 67-96.

Elliot, D., 1972. Deformation paths in structural geology. Geol. Soc. Am. Bull., 83, 2621-2638.

_____ 1976. The energy balance and deformation of thrust sheets. Phil. Trans. R. Soc. Lond. A, 283, 289-312.

Engelder, T. and Engelder, R., 1977. Fossil distortion and decollement tectonics of the Appalachian Plateau. Geology, 5, 456-460.

_____ and Geiser, P., 1979. The relationship between pencil cleavage and lateral shortening within the Devonian section of the Appalachian Plateau, New York. Geology, 7, 460-464.

Fischer, M. W. and Coward, M. P., 1982. Strains and folds within thrust sheets: an analysis of the Heilam sheet, Northwest Scotland. Tectonophysics, 88, 291-312.

Fletcher, R. C. and Pollard, D. D., 1982. Structure of single tectonic solution surfaces: implications for the mechanics of "anticracks". Geol. Soc. Am. Absts. w/ Progs., 14, p. 489.

Frey, M., 1970. The stage from diagenesis to metamorphism in pelitic rocks during Alpine orogenesis. Sedimentology, 15, 261-279.

Gray, D. R., 1981. Compound tectonic fabrics in singly folded rocks from southwest Virginia, U. S. A. Tectonophysics, 78, 229-248.

_____ and Durney, D., 1979. Investigations on the mechanical significance of crenulation cleavage. Tectonophysics, 58, 35-79.

Gwinn, V. E., 1970. Kinematic patterns and estimates of lateral shortening, Valley and Ridge and Great Valley Provinces, Central Appalachians, south-central Pennsylvania. In: G. W. Fisher, F. M. Pettijohn, J. C. Reed Jr. and K. N. Weaver (eds.), Studies of Appalachian Geology: Central and Southern. Interscience, New York, 127-146.

Harris, A. G., Harris, L. D. and Epstein, J. B., 1978. Oil and gas data from the Paleozoic rocks in the Appalachian basin: maps for assessing hydrocarbon potential and thermal maturity (conodont color alteration isograds and overburden isopachs). U.S.G.S. Misc. Invest. Series, Map I-917-E.

Harris, L. D., 1970. Details of thin-skinned tectonics in parts of Valley and Ridge and Cumberland Plateau Provinces of the Southern Appalachians. In: G. W. Fisher, F. M. Pettijohn, J. C. Reed Jr. and K. N. Weaver (eds.), Studies of Appalachian Geology: Central and Southern. Interscience, New York, 161-173.

_____ and Bayer, K. C., 1979. Sequential development of the Appalachian orogen above a master decollement-a hypothesis. Geology, 7, 568-572.

_____ and Milici, R. C., 1977. Characteristics of thin-skinned style of deformation in the southern Appalachians, and potential hydrocarbon traps. U.S.G.S. Prof. Paper 1018, 40 p.

Hoffman, J. and Hower, J., 1979. Clay mineral assemblages as low grade metamorphic geothermometers: application to the thrust faulted disturbed belt of Montana, U. S. A. S.E.P.M. Spec. Publ. 26, 55-79.

Hossack, J. R., 1978. The correction of stratigraphic sections for tectonic finite strain in the Bygdon area, Norway. J. Geol. Soc. Lond., 135, 229-241.

House, W. and Gray, D., 1982. Displacement transfer at thrust terminations in southern Appalachians - Saltville Thrust as an example. A.A.P.G. Bull., 48:7, 830-842.

Kerrich, R., Beckinsale, R. D. and Shackleton, N. J., 1978. The physical and hydrothermal regime of tectonic vein systems: evidence from stable isotope and fluid inclusion studies. N. Jb. Miner. Abh., 131, 225-239.

Kisch, H. J., 1980. Incipient metamorphism of Cambro-Silurian clastic rocks from the Jamtland Supergroup, Central Scandinavian Caledonides, Western Sweden: illite crystallinity and "vitrinite" reflectance. J. Geol. Soc. Lond., 137, 271-288.

Kligfield, R., 1983. Fold propagation and the development of pressure solution and vein features in thrust systems. Geol. Soc. Am. Absts. w/ Progs., 15:6, p. 615.

Knipe, R. J., 1981. The interaction of deformation and metamorphism in slates. Tectonophysics, 78, 249-272.

Kubler, B., 1964. Les argiles, indicateurs de metamorphisme. Revue Inst. fr. Petrole, 19, 1093-1113.

_____ 1968. Evaluation quantitative du metamorphisme par la cristallinite de illite. Etat des progres realises ces dernieres annees. Bull. Centre Rech. Pau-S.N.P.A., 2, 385-397.

Love, L. G., 1957. Micro-organisms and the presence of syngenetic pyrite. Quart. J. Geol. Soc., 113, 429-440.

Lowry, W. D., 1971. Appalachian overthrust belt, Montgomery County southwest Virginia. Fldtrp. 4 in, Lowry, W. D. (ed.), Guidebook to Appalachian tectonics and sulfide mineralization of southwest Virginia. Virginia Polytechnic Institute and State University Gdbk. 5, 178 p.

_____ 1979. Nature of thrusting along the Allegheny front near Pearisburg and of overthrusting in the Blacksburg-Radford area of Virginia. Virginia Polytechnic Institute and State University Guidebook 8, 66 p.

Marshak, S., 1982. The role of clay in strain partitioning in low-grade carbonate rocks. Geol. Soc. Am. Absts. w/ Progs., 14, p. 556.

Milici, R. C., Harris, L. D., and Statler, A. T., 1979. An interpretation of seismic cross sections in the Valley and Ridge of eastern Tennessee. Tennessee Div. Geol., Oil and Gas Seismic Inv. Ser. 1, 2 sheets.

Morse, J. D., 1977. Deformation in ramp regions of overthrust faults: experiments with small-scale rock models. In: Twenty-ninth Annual Field Conference-1977 Wyoming Geol. Ass. Gdbk., 457-470.

Perry, W. J., Jr., 1978. Sequential deformation in the Central Appalachians. Am. J. Sci., 278, 518-542.

Pique, A., 1982. Relations between stages of diagenetic and metamorphic evolution and the development of a primary cleavage in the Northwestern Moroccan Meseta. J. Struct. Geol., 4:4, 491-500.

Powell, C. McA., 1979. A morphological classification of rock cleavage. Tectonophysics, 58, 21-34.

Price, R. A., 1967. The tectonic significance of mesoscopic subfabrics in the southern Rocky Mountains of Alberta and British Columbia. Can. J. Earth Sci., 4, 39-70.

Ramsay, J. G., 1967. Folding and Fracturing of Rocks. McGraw-Hill, New York.

_____, Casey, M. and Kligfield, R., 1983. Role of shear in development of Helvetic fold- thrust belt of Switzerland. Geology, 11, 439-442.

Rattey, P. R. and Sanderson, D. J., 1982. Patterns of folding within nappes and thrust sheets: examples from the Variscan of Southwest England. Tectonophysics, 88, 247-267.

Read, J. F., 1980. Carbonate ramp-to-basin transitions and foreland basin evolution, Middle Ordovician, Virginia Appalachians. A.A.P.G. Bull., 64:10, 1575-1612.

Reks, I. J. and Gray, D. R., 1982. Pencil structure and strain in weakly deformed mudstone and siltstone. J. Struct. Geol., 4:3, 161-176.

Rich, C. I., 1969. Suction apparatus for mounting clay specimens on ceramic tile for X-ray diffraction. Soil Sci. Soc. Proc., 33, 815-816.

Rich, J. L., 1934. Mechanics of low-angle overthrust faulting as illustrated by Cumberland Thrust Block, Virginia, Kentucky, and Tennessee. A.A.P.G. Bull., 18:12:7, 1584-1596.

Rodgers, J., 1970. The tectonics of the Appalachians. Wiley-Interscience, New York, 271 p.

Roeder, D., Yust, W. W. and Little, R. L., 1978. Folding in the Valley and Ridge Province of Tennessee. Am. J. Sci., 278, 477-496.

Roeder, D., Gilbert, O. E., Jr. and Witherspoon, W. D., 1978. Evolution and macroscopic structure of Valley and Ridge thrust belt, Tennessee and Virginia. Dept. of Geol. Sci.; Univ. of Tennessee, Knoxville. Studies in geology 2, 25 p.

Sanderson, D. J., 1982. Models of strain variation in nappes and thrust sheets: a review. Tectonophysics, 88, 201-233.

Schultz, A. P., 1979. Deformation associated with Pulaski overthrusting in the Price Mountain and East Radford windows, Montgomery County, Virginia. Unpubl. M. S. thesis, Virginia Polytechnic Institute and State University, Blacksburg, Virginia, 134 p.

_____ 1983. Broken formations of the Pulaski thrust sheet near Pulaski, Virginia. Unpubl. Ph. D. thesis, Virginia Polytechnic Institute and State University, Blacksburg, 82 p.

Selkman, S. O., 1983. Stress and displacement distributions around pyrite grains. J. Struct. Geol., 5:1, 47-52.

Serra, S., 1977. Styles of deformation in the ramp regions of overthrust faults. In: Twenty-ninth Annual Field Conference-1977 Wyoming Geol. Ass. Gdbk., 487-498.

Siddans, A. W. B., 1977, The development of slaty cleavage in a part of the French Alps. Tectonophysics, 39, 533-557.

Simon, R. I. and Gray, D. R., 1982. Interrelations of mesoscopic structures and strain across a small regional fold, Virginia Appalachians. J. Struct. Geol., 4:3, 271-289.

Spears, D. B., 1983. Strain in Ordovician and Devonian shales from the Massanutten Synclinorium - implications for fold development and tectonic history. Unpubl. M. S. thesis, Virginia Polytechnic Institute and State University, Blacksburg, Virginia, 70 p.

Spry, A., 1969. Metamorphic textures. Pergamon Press, London, 350 p.

Stanley, C. B., 1983. Kinematic implications of footwall structures. Unpubl. M. S. thesis, Virginia Polytechnic Institute and State University, Blacksburg, Virginia, 71 p.

Stevenson, J. J., 1885. Notes on the geologic structure of Tazwell, Russell, Wise, Smyth and Washington Counties of Virginia. Am. Philos. Soc. Pr., 22, p. 121.

Velde, B., 1977. Clays and clay minerals in natural and synthetic systems. Elsevier Scientific, Amsterdam, 218 p.

Weaver, C. E., 1960. Possible uses of clay minerals in search for oil. A.A.P.G. Bull., 44, 1505-1518.

_____ 1961. Clay minerals of the Ouachita structural belt and adjacent foreland. In: The Ouachita System. The Univ. Texas Publ. 6120, Bureau Econ. Geol. Austin, TX, 147-160.

_____, Beck, K. C. and Pollard, C. O., Jr., 1971. Clay water diagenesis during burial: how mud becomes gneiss. Geol. Soc. Am. Spec. Paper 134, 96 p.

Webb, F., Jr., 1959. Geology of the Middle Ordovician limestones in the Rich Valley area, Smyth County, Virginia. Unpubl. M. S. thesis, Virginia Polytechnic Institute and State University, Blacksburg, Virginia, 96 p.

_____ 1965. Geology of the Big Walker Mountain - Crockett Cove area, Bland, Pulaski, and Wythe Counties, Virginia. Unpubl. Ph. D. thesis, Virginia Polytechnic Institute and State University, Blacksburg, Virginia, 171 p.

Weber, K., 1972. Notes on determination of illite crystallinity. N. Jb. Miner. Abh., 6, 267-276.

_____ 1981. Kinematic and metamorphic aspects of cleavage formation in very low-grade metamorphic slates. Tectonophysics, 78, 291-306.

White, S. H. and Johnston, D. C., 1981. A microstructural and microchemical study of cleavage lamellae in a slate. J. Struct. Geol., 3:3, 279-290.

White, S. H. and Knipe, R. J., 1978. Microstructure and cleavage development in selected slates. Contrib. Mineral. Petrol., 66, 165-174.

Wickham, J. S., 1973. An estimate of strain increments in a naturally deformed carbonate rock. Am. J. Sci., 273, 23-47.

_____ and Anthony, M, 1977. Strain paths and folding of carbonate rocks near Blue Ridge, central Appalachians. Geol. Soc. Am. Bull., 88, 920-924.

Wiltschko, D. V., 1978. A mechanical model for thrust sheet deformation at a ramp. J. Geophys. Res., 84, 1091- 1104.

_____ 1981. Thrust sheet deformation at a ramp: summary and extensions of an earlier model. In: K. R. McClay and N. J. Price (eds.), Thrust and Nappe Tectonics. Geol. Soc. Lond. Spec. Publ. 9, 55-63.

Winsor, C. N., 1983. Syntectonic vein and fibre growth associated with multiple slaty cleavage development in the Lake Moondarra area, Mount Isu, Australia. Tectonophysics, 92, 195-210.

Wojtal, S. F., 1982. Finite deformation in thrust sheets and their material properties. Unpubl. Ph. D. thesis, Johns Hopkins University, Baltimore, Maryland, 313 p.

Woodland, B. G., 1982. Gradational development of domainal slaty cleavage, its origin and relation to chlorite porphyroblasts in the Martinsburg Formation, eastern Pennsylvania. Tectonophysics, 82, 89-124.

_____ 1983. Mineralogy and structural relationships of cleavage in the Twin Creek Formation within part of the Crawford thrust sheet in Wyoming and Idaho. Unpubl. M. S. thesis, University of Wyoming, Laramie, Wyoming, 125 p.

end

APPENDIX A. STRAIN

STRAIN MEASUREMENT

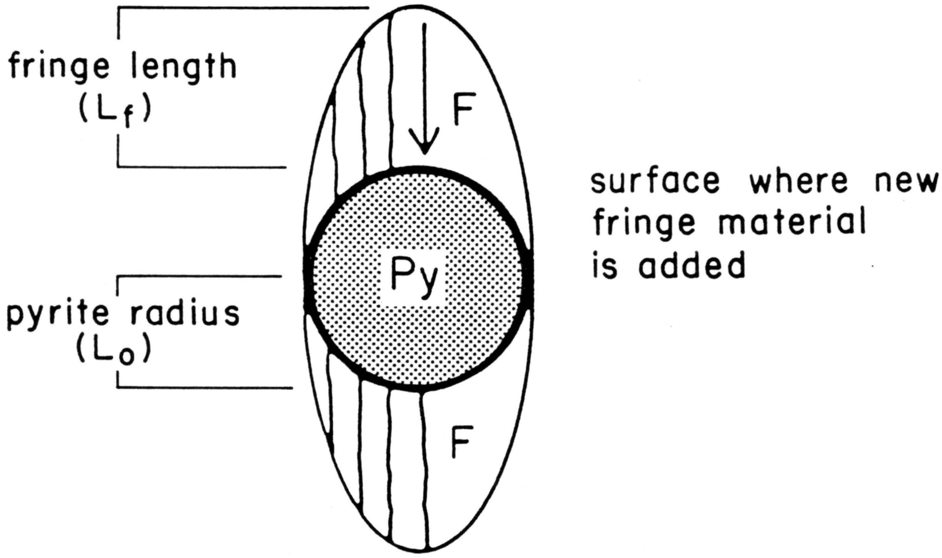

F = pressure fringe

Py = frambodial pyrite

Arrow indicates direction of progressive fiber growth during antitaxial growth.

Determination of e_1 *

$$\boxed{e_1 = L_f / L_o = \text{fringe length} / \text{pyrite radius}}$$

Assuming plane strain: $1 + e_2 = 1$, and $1 + e_3 = 1/(1 + e_1)$

* for straight fibers

Strain Data
NE-trending S1 Cleavage

*Sample	Pyrite Dia.(μ)	$1+e_1$	$1+e_3$	Mean $(1+e_1)$	Standard Deviation
DM-03	22.0	2.17	0.462	2.23	0.085
	25.6	2.29	0.438		
DM-06	20.1	2.27	0.440	2.15	0.207
	22.0	2.33	0.429		
	25.6	2.14	0.467		
	36.6	1.80	0.555		
	45.8	2.20	0.455		
DM-17	25.2	2.71	0.369	2.16	0.232
	27.5	1.93	0.517		
	27.5	2.47	0.405		
	27.5	2.06	0.485		
	28.8	2.13	0.469		
	34.8	2.16	0.463		
	34.8	2.32	0.431		
	38.4	1.76	0.568		
	40.3	2.09	0.478		
	43.2	2.16	0.463		
	46.8	1.92	0.521		
	64.1	2.14	0.467		
	64.8	2.11	0.474		
	68.4	2.26	0.442		
	72.0	2.40	0.417		
	72.0	2.00	0.500		
	466.7	2.22	0.450		
DM-200	16.5	2.33	0.429	2.08	0.242
	18.3	2.40	0.417		
	20.1	2.45	0.407		
	25.6	2.14	0.466		
	27.5	1.93	0.517		
	27.5	1.67	0.599		
	27.5	2.47	0.405		
	27.5	2.14	0.467		
	29.3	2.13	0.471		
	31.1	2.18	0.459		
	31.1	1.94	0.515		
	31.1	2.29	0.436		
	32.9	2.11	0.474		
	34.8	2.11	0.475		
	36.6	2.00	0.500		
	40.3	2.09	0.478		
	43.9	1.58	0.633		

Sample	Pyrite Dia. (μ)	$1+e_1$	$1+e_3$	Mean $(1+e_1)$	Standard Deviation
DM-200A	12.8	2.71	0.369	2.55	0.185
	14.6	2.75	0.420		
	18.3	2.40	0.416		
	19.2	2.14	0.466		
	22.0	2.83	0.353		
	25.6	2.43	0.412		
	25.6	2.71	0.368		
	29.3	2.55	0.391		
	40.3	2.36	0.424		
	43.9	2.42	0.414		
DM-201	32.9	3.44	0.291	2.41	0.347
	32.9	2.55	0.391		
	34.8	2.26	0.442		
	37.0	3.00	0.333		
	37.0	1.80	0.556		
	37.0	2.60	0.385		
	47.6	2.31	0.433		
	51.8	2.71	0.361		
	54.9	3.13	0.319		
	56.7	2.23	0.449		
	59.2	2.25	0.440		
	59.2	2.37	0.421		
	60.4	2.33	0.429		
	70.3	2.26	0.442		
	77.7	1.95	0.513		
	79.2	2.64	0.379		
	96.2	2.23	0.448		
	96.2	2.23	0.448		
DM-201A	29.6	2.50	0.400	2.56	0.270
	37.0	2.40	0.417		
	37.0	2.20	0.455		
	51.8	2.43	0.412		
	51.8	2.43	0.412		
	59.2	2.75	0.364		
	66.6	2.66	0.376		
	73.2	2.75	0.364		
	74.0	2.80	0.357		
	74.0	2.60	0.385		
	81.4	2.09	0.478		
	81.4	2.09	0.478		
	88.8	3.00	0.333		

Sample	Pyrite Dia.(μ)	$1+e_1$	$1+e_3$	Mean $(1+e_1)$	Standard Deviation
DM-211	31.1	2.29	0.437	2.44	0.267
	42.1	2.65	0.377		
	43.9	2.25	0.444		
	49.4	2.33	0.429		
	56.7	2.29	0.437		
	60.4	2.21	0.452		
	62.2	2.29	0.437		
	62.2	2.35	0.426		
	73.2	2.30	0.435		
	88.8	2.92	0.342		
	103.6	2.43	0.412		

NW-trending S2 Cleavage

Sample	Pyrite Dia.(μ)	$1+e_1$	$1+e_3$	Mean $(1+e_1)$	Standard Deviation
DM-107	23.8	2.23	0.448	2.22	0.289
	25.6	2.57	0.389		
	29.3	2.25	0.444		
	47.7	2.23	0.448		
	54.9	2.33	0.429		
	64.1	1.69	0.593		
DM-109	25.6	1.86	0.538	1.82	0.064
	47.6	1.77	0.565		
DM-113	16.5	2.33	0.429	1.61	0.057
	22.0	1.67	0.600		
	29.3	1.56	0.640		
	31.1	1.59	0.630		
DM-115	12.8	2.43	0.412	2.10	0.084
	18.3	2.20	0.455		
	22.0	2.00	0.500		
	25.6	2.14	0.467		
	47.6	2.15	0.464		
DM-118	14.6	2.25	0.444	1.83	0.023
	23.8	1.62	0.619		
	25.6	1.86	0.538		
	31.1	1.82	0.548		
	31.1	1.82	0.548		
DM-119	38.4	1.67	0.600	1.78	0.108
	40.3	1.73	0.579		
	42.1	1.87	0.535		
	47.6	1.85	0.542		
DM-122	22.9	1.64	0.610	1.57	0.122
	31.1	1.71	0.586		
	40.3	1.46	0.688		
	42.1	1.48	0.676		
DM-139	38.4	1.86	0.538	1.70	0.174
	42.1	1.61	0.622		
	62.9	2.06	0.485		
	64.1	1.57	0.636		
	85.1	1.74	0.545		
	87.8	1.58	0.632		
	95.2	1.56	0.634		
	96.2	1.62	0.617		

Sample	Pyrite Dia. (μ)	$1+e_1$	$1+e_3$	Mean $(1+e_1)$	Standard Deviation
DM-139 (cont.)	96.2	1.85	0.542		
	97.0	1.53	0.654		
	102.5	1.57	0.636		
DM-142	21.6	1.80	0.555	1.81	0.054
	27.0	1.80	0.555		
	28.8	1.88	0.533		
	29.3	1.75	0.571		
DM-148A	14.6	2.13	0.471	2.03	0.244
	18.3	1.60	0.625		
	18.3	2.20	0.455		
	27.5	2.14	0.466		
	31.1	1.75	0.571		
DM-149	23.8	1.92	0.521	2.14	0.246
	23.8	1.92	0.521		
	25.6	2.00	0.500		
	32.9	2.11	0.474		
	36.6	2.00	0.500		
	36.6	2.45	0.408		
	36.6	2.40	0.417		
	40.3	2.14	0.467		
	47.6	1.85	0.542		
	49.4	1.96	0.509		
	92.5	2.56	0.391		
DM-150	18.3	1.60	0.625	1.66	0.325
	18.3	1.80	0.556		
	20.1	1.91	0.524		
	21.1	2.22	0.450		
	28.4	1.71	0.585		
	29.3	1.50	0.667		
	29.3	1.50	0.667		
	58.6	1.31	0.762		
	60.4	1.33	0.750		
	66.6	1.67	0.600		
DM-153	21.6	2.16	0.463	2.06	0.220
	27.0	2.20	0.455		
	28.8	2.00	0.500		
	40.3	1.91	0.524		
	40.7	2.09	0.478		
	43.2	1.67	0.600		
	55.5	1.93	0.518		
	59.2	2.16	0.463		
	79.2	2.45	0.407		

Sample	Pyrite Dia.(μ)	$1+e_1$	$1+e_3$	Mean $(1+e_1)$	Standard Deviation
DM-155	22.0	1.62	0.619	1.61	0.010
	23.8	1.62	0.619		
	54.0	1.60	0.625		
	56.7	1.61	0.623		
DM-173	36.6	1.70	0.588	1.57	0.191
	51.2	1.43	0.700		
	120.8	1.33	0.750		
	170.2	1.31	0.763		
DM-178	23.8	1.92	0.520	1.94	0.257
	27.5	2.13	0.471		
	29.3	2.25	0.444		
	31.1	1.94	0.515		
	36.6	1.50	0.667		
	62.2	1.88	0.531		
DM-194B	20.1	2.22	0.451	2.23	0.014
	40.3	2.24	0.441		
DM-207	22.0	2.33	0.429	2.23	0.085
	25.6	2.29	0.438		
	27.5	2.20	0.455		
	33.9	2.11	0.474		
	38.4	2.24	0.446		
DM-217	31.1	1.59	0.630	1.58	0.012
	31.1	1.59	0.630		
	51.2	1.57	0.636		
DM-239	38.4	1.67	0.600	1.56	0.158
	51.2	1.64	0.609		
	59.2	1.75	0.571		
	60.4	1.42	0.702		
	60.4	1.30	0.769		
	71.4	1.62	0.619		
	74.0	1.50	0.667		
	74.0	1.50	0.667		
	103.6	1.29	0.775		
	148.0	1.30	0.769		
	148.0	1.40	0.714		
	162.8	1.27	0.787		
DM-242	67.7	1.34	0.745	1.36	0.021
	69.5	1.37	0.731		
	102.5	1.34	0.747		

Sample	Pyrite Dia.(μ)	$1+e_1$	$1+e_3$	Mean $(1+e_1)$	Standard Deviation
DM-246	25.6	2.00	0.500	1.97	0.165
	31.1	2.06	0.486		
	32.9	2.16	0.462		
	36.6	1.80	0.556		
	45.8	1.80	0.556		
	45.8	1.80	0.556		
	47.6	2.15	0.465		
DM-325	36.0	1.60	0.625	1.58	0.074
	43.2	1.67	0.600		
	57.6	1.50	0.667		
	93.6	1.54	0.650		
DM-331	12.8	2.14	0.467	2.15	0.021
	14.6	2.00	0.500		
	16.5	2.22	0.450		
	22.0	2.16	0.462		
	29.3	2.13	0.471		

*Sample locations are on base maps filed in the Orogenic Studies Laboratory, Department of Geological Sciences, Blacksburg, Virginia 24061.

APPENDIX B. PHYLLOSILICATE MINERALOGY

Phyllosilicate mineralogy of the spaced cleavage in the Ordovician Rich Valley and Moccasin Formations was determined by X-ray diffraction analysis using a Dyano XRD-8300 diffractometer. Operating parameters were: copper K-alpha radiation (40 kV, 30mA); diffraction slit width=0.2 mm; goniometer rate=2° 2θ/minute; recording chart rate=20 cm/hr./. Sample preparation and X-ray diffraction analysis procedures are listed below.

1. Mechanical disaggregation. Carbonate mudrock samples were mechanically crushed; particle size was reduced to approximately 0.6 mm in diameter.

2. Carbonate removal. Using 1N NaOAc solution buffered at approximately pH=5.0.

3. Pyrite removal. Using 30% H_2O_2 solution (80°C). PH was raised to approximately 8.0 using Na_2CO_3.

4. Free iron oxide removal. Using 0.3 M Na citrate solution, 1.0 M $NaHCO_3$ solution, and Na_2CO_3 solid.

5. Particle size fractionation. Separation of sand-size fraction (>50μ) using a 300-mesh sieve. Separation of

silt-size (50μ-2μ) and clay-size (<2μ) fractions through flocculation and controlled centrifugation.

6. Tile preparation. Suspension containing clay-size fraction (<2μ) was pipetted on to two (2) unglazed ceramic tiles mounted in a suction device (Rich, 1969). One tile was washed five (5) times with 1 N $MgCl_2$ solution, the other five (5) times with 1 N KCl solution, to ensure cation saturation. Tiles were rinsed with deionized water to remove excess ions. Mg saturated tiles were subsequently washed with a dilute glycerol solution (for identification of expandable species).

7. X-ray diffractometry. Dry samples were analyzed on the diffractometer between 2° and 32° 2θ at 25°C, 110°C, 300°C and 550°C. Several samples were analyzed by differential scanning calimetry from 25° to 600°C to check for the presence of kaolinite. For determination of illite crystallinity each sample was run through X-ray diffraction scans from 8° to 12° 2θ giving the 10A peak (001) of illite. The recording chart rate was increased to 120 cm/hr. to produce wider 10A peaks.

Identification of clay minerals was based on X-ray diffraction patterns of K and Mg saturated tile mounts and their behavior with heat treatments. A typical diffraction pattern is shown on the following page.

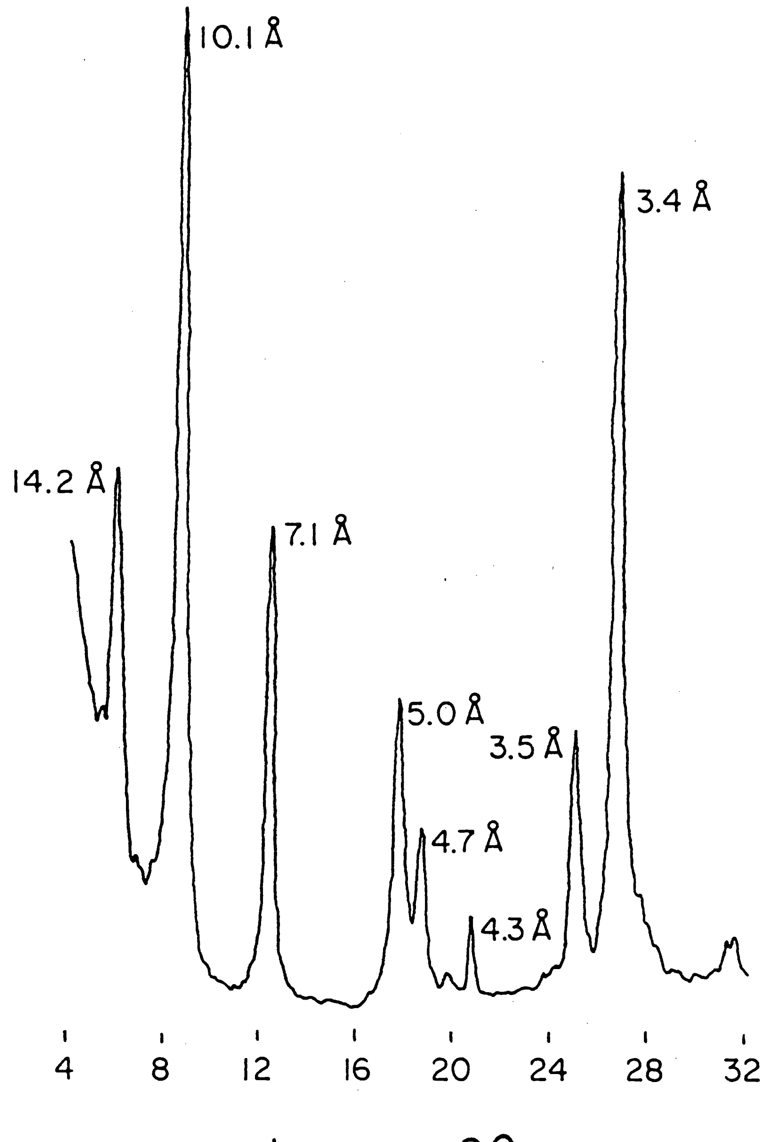

Representative X-ray diffraction pattern. Mg saturated tile at 25°C.

X-RAY DIFFRACTION DATA

Sample	Illite Crystallinity $H^{10A}/H^{10.5A}$	Hb(mm)	$I^{(002)}/I^{(001)}$ (10A peak)	$I^{(002)}/I^{(001)}$ (14A peak)
MC-101	2.58	11.50	0.34	1.55
MC-108	2.76	9.75	0.42	2.48
MC-126	2.27	11.00	0.34	1.77
RV-03	2.98	11.00	0.42	0.62
RV-107	1.93	13.00	0.41	0.39
RV-114	2.92	9.50	0.33	0.25
RV-149	2.21	12.00	0.34	2.30
RV-194	1.99	10.75	0.41	1.45
RV-214	3.41	8.50	0.40	1.34
RV-242	2.81	12.75	0.38	0.29
RV-245	1.74	16.75	0.33	0.21
RV-331	2.38	11.50	0.40	2.60

H^{10A}, $H^{10.5A}$=height of illite peak at 10A and 10.5A respectively
Hb=width of 10A peak at half-height
I=integrated intensity

APPENDIX C. PRESSURE SOLUTION DATA

Sample	F(wt.%)	L^f(mm)	L^m(mm)	L^o(mm)	L(mm)	e_3
MC-101	0.144	24	276	442	300	0.322
MC-108	0.167	38	262	490	300	0.387
MC-126	0.162	32	268	466	300	0.356
RV-03	0.129	31	269	509	300	0.411
RV-107	0.134	36	264	543	300	0.448
RV-114	0.154	31	269	470	300	0.326
RV-149	0.183	34	266	452	300	0.336
RV-194	0.097	25	275	533	300	0.437
RV-214	0.131	26	274	472	300	0.365
RV-242	0.142	11	289	367	300	0.181
RV-245	0.168	09	289	345	300	0.129
RV-331	0.179	43	257	497	300	0.391

F=weight percent insolubles

L^f=cumulative width of cleavage folia along traverse

L^m=cumulative width of microlithons along traverse

L^o=length prior to deformation (calculated)

L=length of traverse

Note - thin sections were projected and enlarged for measurement

The vita has been removed from the scanned document

Geologic Map and Cross Section of the Southwestern End of Wallker Mountain, Southwestern Virginia

David Monz, Lynn Glover, III and Fred Webb*

Orogenic Studies Laboratory
Department of Geological Sciences
Virginia Tech, Blacksburg, Va.

*Department of Geology
Appalachian State University, Boone, N.C.

1984

STRATIGRAPHY

DEVONIAN

- **Dun** — Devonian Undifferentiated: Millboro Fm.- black fissile shale; Brallier Fm.- thin-bedded sandstone and siliceous gray shale. Chemung Fm.- medium-bedded sandstone and yellow-brown shale.
- **Dh** — Huntersville Chert: irregularly bedded, gnarled black chert with sparse sandstone and shale interbeds.

UNCONFORMITY - increasing in magnitude from NE to SW

SILURIAN

- **St** — Tuscarora Fm.: white to light gray, medium-grained, cross-bedded quartzite.

ORDOVICIAN

- **Oj** — Juniata Fm.: dark red, medium-bedded sandstone with minor red and green shale and siltstone interbeds.
- **Omb** — Martinsburg Fm.: interbedded dark gray, thin-bedded, coarse-grained skeletal limestone, brown sandstone, and yellow-brown shale and siltstone.
- **Om / Omw** — Moccasin Fm. (Om): red calcareous mudrock, argillaceous limestone and pelletal limestone; well-developed penetrative to spaced cleavage. Walker Mtn. sandstone member (Omw): white to gray, medium-grained, conglomeratic quartzite.
- **Ow** — Wassum Fm.: light gray skeletal grainstone and shaly pelletal to nodular limestone; local cleavage development.
- **Orv** — Rich Valley Fm.: black calcareous shale and limestone; well developed penetrative to spaced cleavage.
- **Oe** — Effna Fm.: light gray skeletal grainstone and wackestone.
- **Ol** — Lenoir Fm.: gray, medium- to thick-bedded skeletal grainstone and packstone with silty dolomite stringers. Localized gray skeletal grainstone and fine-grained sandstone at base.

KNOX UNCONFORMITY

- **C-Ok** — Knox Gp.: Lower Knox- gray, thin- to thick-bedded stromatolithic dolomite with minor interbedded sandstones; Upper Knox- gray, medium- to thick-bedded cherty dolomite with limestone interbeds.

CAMBRIAN

SALTVILLE SHEET

- **Cn** — Nolichucky Fm.: limestone-dolomite ribbon rock, calcareous shale and siltstone.
- **Ch** — Honaker Fm.: gray, thick- to massively-bedded, fine- to medium-grained dolomite.

PULASKI SHEET

- **Ce** — Elbrook Fm.: gray, thick- to massively-bedded dolomite, locally argillaceous, with sparse limestone interbeds.

STRUCTURAL DATA

- strike and dip of bedding
- strike and dip of overturned bedding
- strike and dip of S_1 cleavage
- strike and dip of S_2 cleavage
- trend and plunge of micro-fold axes (folded S_1 cleavage)
- trend and plunge of mesoscopic fold axes
- trend and plunge of regional anticline
- trend and plunge of regional syncline
- trend and plunge of regional overturned syncline

CONTACTS

- known
- approximate

FAULTS

- known
- approximate
- inferred

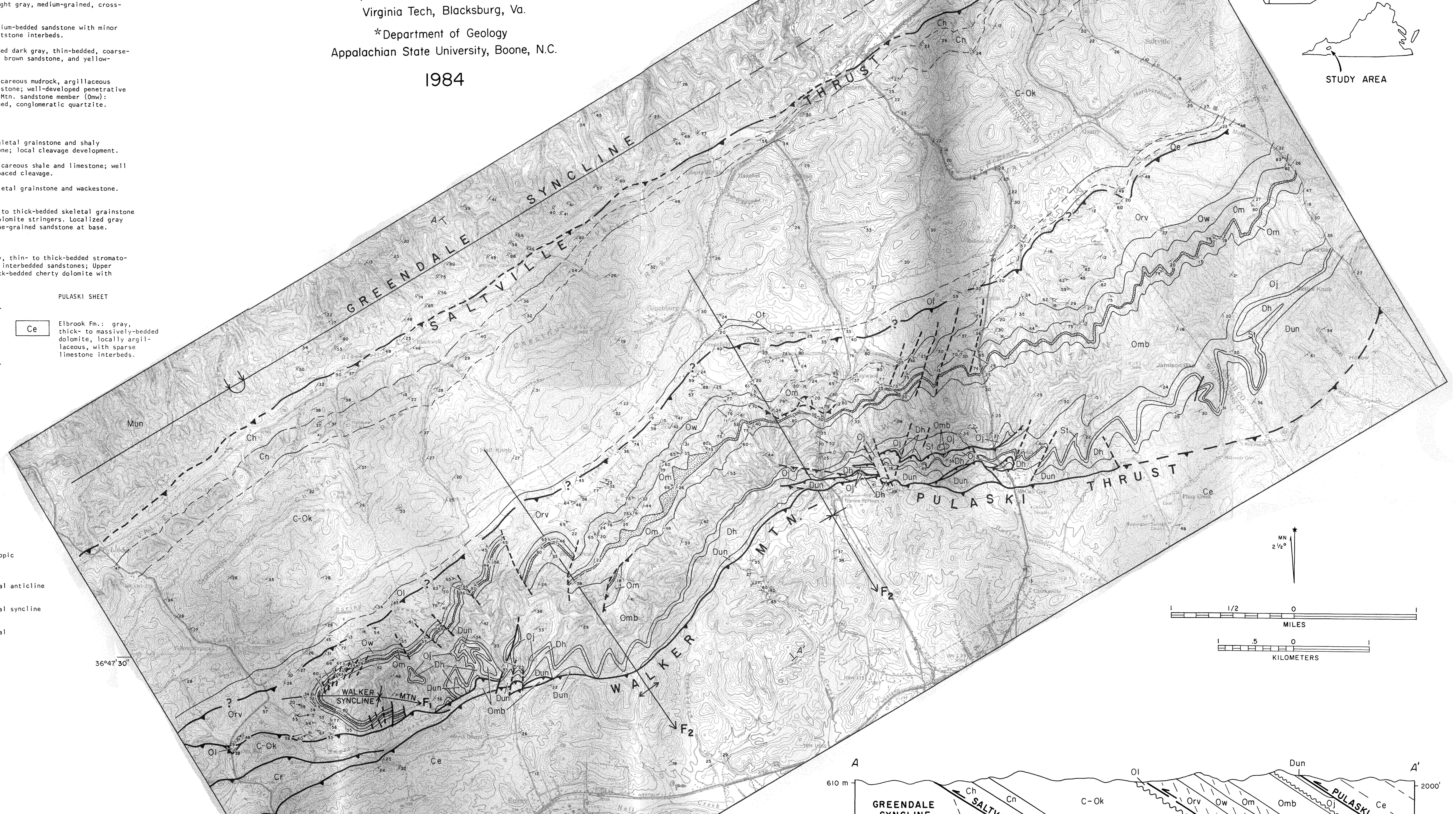

QUADRANGLES